



AMERICAN UNIVERSITY OF BEIRUT

UNDERSTANDING THE ROLE OF CERAMIDE IN p53-  
MEDIATED AND p53-INDEPENDENT RESPONSES TO  
HYPOXIA IN HCT-116 COLON CANCER CELLS

by  
KAREN MAROUN MECHLEB

A thesis  
Submitted in partial fulfillment of the requirements  
for the degree of Master of Science  
to the Department of Biochemistry and Molecular Genetics  
of the Faculty of Medicine  
at the American University of Beirut

Beirut, Lebanon  
June, 2020

AMERICAN UNIVERSITY OF BEIRUT

UNDERSTANDING THE ROLE OF CERAMIDE IN  
p53-MEDIATED AND p53-INDEPENDENT  
RESPONSES TO HYPOXIA IN HCT-116 COLON  
CANCER CELLS

By

KAREN MAROUN MECHLEB

Approved by:



Dr. Ghasan Dbaibo, MD  
Professor, Biochemistry and Molecular Genetics

Advisor



Dr. Nadine Darwiche  
Professor; Biochemistry and Molecular Genetics

Member of Committee



Dr. Pierre Khoueiry  
Assistant Professor, Biochemistry and Molecular Genetics

Member of Committee



Dr. Nathalie Khoueiry-Zgheib  
Associate Professor, Pharmacology and Toxicology

Member of Committee

Date of thesis/dissertation defense: [June 18, 2020]



## ACKNOWLEDGMENT

First and foremost, with sincere praises, I thank God for being there in every step of my research study, for giving me strength, knowledge, and ability to complete my thesis work. For my angel in heaven, thank you for watching me and continuously praying for me from above. Without your immense grace, this achievement would have not been possible.

Second to none, to my advisor, Dr. Ghassan Dbaibo thanks for giving me the opportunity to pursue my Master's thesis project in your laboratory and for believing in my potentials. Thank you for providing me with the most beneficial advices which guided my project to the right direction. I'm so grateful that I had the chance to have you as my mentor.

To Dr. Marguerite Mrad Kassab, you are a true role model. Your guidance helped me in all the time of research and writing of this thesis. I really appreciate the immense knowledge, the continuous support, patience, and motivation, you have given me during this year and the trust you have put in my work.

To the sweetest Nancy Hourany, I owe you a lot. I have not only gained experience on a technical level by the time we spent together, but also a friend who has a heart of gold. Thank you very much.

To my friends and daily supporters: Lara Daou, Zainab Abdel Ghani, Jessica Halimeh, Christelle Abi Khalil, Hasan Hijazi and Marc Finianos; thank you for always being there and for all the positive and relieving thoughts you have given me.

To the sweetest Mrs. Rania Shatila and Mr. Joan Younes, thank you for providing me with continuous help and support through my work in the flow cytometry facility.

To my very precious ones, Perla Mechleb and Peter Assaf, many thanks for being in my life. I am so grateful for the unfailing support and continuous encouragement you provided me throughout my years of study and through all my ups and downs. Without your support, I would have never succeeded. A thank you is never enough!

Above ground, I am indebted to my very special family for your continuous support; I would have never been this strong without you as my inspiration. You are the reason why I keep pushing; I keep facing all the struggles and hardships. Your unconditional love and belief in my potentials have been the most rewarding.

## AN ABSTRACT OF THE THESIS OF

Karen Maroun Mechleb

for

Master of Science

Major: Biochemistry and  
Molecular Genetics

Title: Understanding the role of ceramide in p53-mediated and p53-independent responses to hypoxia in hct-116 colon cancer cells

Hypoxia is a common feature of solid tumors resulting from the disordered vasculature developed to supply oxygen to the rapidly growing tumor. As a result, gradients of oxygen concentration emerge; regions of severe hypoxia undergo cell death through the stabilization and activation of p53. Cancer cells can evade hypoxia-induced cell death by inducing genetic alterations, such as mutations in the *TP53* tumor-suppressor gene. Hypoxic stress then acts as a potent selector for aggressive mutant clones allowing their expansion at the expense of their wild-type hypoxia-sensitive counterparts. Restoration of hypoxia-induced apoptosis in tumors harboring p53 mutations has been proposed as a potential therapeutic strategy. Although several p53-targeted therapies have entered clinical trials, several limitations arose and hindered the efficacy of these approaches.

Ceramide, a signaling sphingolipid, was previously reported as a potential collaborator with p53 in the stress-induced cellular response. Ceramide metabolism is quite complex and comprises a set of reactions that produce different metabolites involved in a variety of cellular responses. While ceramide (Cer) and sphingosine (Sph) act as pro-apoptotic lipids, ceramide 1-phosphate (C1P) and sphingosine 1-phosphate (S1P) are considered as oncometabolites. Slight changes in the balance between pro and anti-apoptotic sphingolipids, commanded by the expression and activity of appropriate enzymes, could dictate cell fate in response to hypoxia in both p53-proficient and p53-deficient cells.

In order to define the role of ceramide in the p53-dependent and independent responses to hypoxia, HCT-116 colon carcinoma cells differentially expressing p53 were incubated under 1% O<sub>2</sub> and the changes in their ceramide metabolism were measured at several time points. Unlike p53-proficient colonic carcinoma HCT-116 cells, p53-deficient cells resisted the apoptotic response induced by hypoxia. This resistance was accompanied by ceramide accumulation and a drop in sphingosine levels, which may have been promoted by sphingosine phosphorylation into the anti-apoptotic sphingolipid S1P. Indeed, we showed, through protein and mRNA expression studies as well as through enzymatic pharmacological modulation, that ceramide synthases and

dihydroceramide desaturase 1, key players in the *de novo* synthesis pathway of ceramide, were orchestrating the response of HCT-116 cells to hypoxia in the absence of p53. We also demonstrated that the drop in sphingosine level upon hypoxia was accompanied by an increase in the mRNA expression of sphingosine kinase 1 in p53-deficient cells, which may have contributed to their resistance to hypoxia-induced apoptosis.

Treating HCT-116 cells with exogenous C6 ceramide specifically targeted p53-deficient cells towards apoptosis, possibly by shifting the ceramide/S1P balance towards ceramide accumulation.

This data supports the hypothesis that bypassing p53 loss of function through altering downstream ceramide metabolism is a potentially promising therapeutic strategy for the treatment of p53-mutated chemo-resistant solid tumors.

# CONTENT

ACKNOWLEDGMENT .....	V
AN ABSTRACT OF THE THESIS OF.....	VI
ILLUSTRATION .....	XII
TABLES .....	XIV
ABBREVIATIONS .....	XV

## Chapter

I. INTRODUCTION.....	1
A. <i>Colon Cancer</i> .....	1
1. Epidemiology and risk factors.....	1
2. Colon carcinogenesis and genetic basis .....	2
B. <i>TP53</i> a tumor suppressor gene.....	3
1. Definition .....	3
2. p53 function.....	4
3. p53 and cell cycle.....	5
4. p53 and apoptosis.....	6
5. p53 and cancer.....	6
6. Targeting p53 .....	7
C. Solid tumors and hypoxia .....	9
1. Solid tumors.....	9
2. Vasculature .....	9



3.	Hypoxia .....	10
4.	Hypoxia Inducible Factors (HIFs) .....	11
5.	Cross-talk between HIF-1 and p53 under hypoxic conditions.....	12
6.	Hypoxia inducible p53 mutation.....	13
7.	Targeting p53 mutation under hypoxic conditions .....	14
D.	Ceramide, a bioactive sphingolipid.....	15
1.	Chemical structure of ceramide .....	15
2.	Bioactive role of ceramide.....	16
3.	Ceramide synthesis.....	16
E.	Inhibitors of ceramide metabolism enzymes .....	22
1.	Fumonisin B1 .....	23
2.	Desipramine.....	24
3.	GW 4869 .....	25
4.	Sphingosine kinase 1 inhibitor SK1-I.....	25
A.	Ceramide.....	25
1.	Ceramide structure-function relationship.....	25
2.	Ceramide: an anti-cancer target.....	26
3.	Ceramide and apoptosis .....	27

Moreover, ceramide can directly bind to the aspartic protease, cathepsin-D (associated with TNF- $\alpha$ , Fas and chemotherapy-induced apoptosis) leading to autolytic cleavage of the pro-enzyme and resulting in its proteolytic activation in the lysosome. This ceramide-induced cathepsin D activation mediates cleavage

and subsequent activation of the pro-apoptotic Bcl-2 family member Bid in response to TNF- $\alpha$ <sup>105</sup> .....	27
4. Ceramide and p53.....	27
5. Ceramide: mediator of the cellular response to hypoxia.....	30
G. Aims of the study:.....	31
<b>II. MATERIALS AND METHODS .....</b>	<b>33</b>
A. Cell culture .....	33
B. Cell viability measurement by MTT .....	33
C. Flow Cytometric Analysis of the DNA Content .....	34
D. Measurement of ceramide levels by DGK assay.....	34
E. Liquid chromatography mass spectrometry (LC/MS).....	35
F. RNA extraction, reverse transcription, and quantitative Real-Time PCR.....	35
1. RNA extraction .....	35
2. Reverse transcription of RNA to cDNA .....	36
3. Quantitative real-time PCR (qRT-PCR).....	36
G. Protein extraction and western blot analysis.....	37
H. Statistical analyses .....	38
<b>III. RESULTS .....</b>	<b>39</b>
A. Defining the role of p53 in the cellular response to hypoxia .....	39
1. Validation of HCT-116 cellular models .....	39

2. Hypoxia-induced response in HCT-116 p53 <sup>+/+</sup> and p53 <sup>-/-</sup> cells.....	40
B. Defining the ceramide response to hypoxia in the presence and absence of p53	
42	
1. Changes in total ceramide levels in response to hypoxia measured by DGK	
assay.....	42
2. Examine the association between ceramide metabolic pathways and the	
biological response to hypoxia .....	44
3. Changes in the levels of ceramide species upon hypoxia .....	55
4. Changes in ceramide catabolism upon hypoxia .....	59
C. Effect of exogenous C6 ceramide on the biological response to hypoxia of HCT-	
116 cells differentially expressing p53 .....	61
<b>IV. DISCUSSION .....</b>	<b>63</b>
<b>V. CONCLUSION AND PERSPECTIVES .....</b>	<b>69</b>
<b>BIBLIOGRAPHY .....</b>	<b>71</b>

## ILLUSTRATION

Figure	Page
1. Molecular events associated with CRC progression.....	3
2. Regulation of p53 and HIF pathways depending on the severity and duration of hypoxia.....	13
3. Chemical structure of ceramide..	16
4. Schematic overview of the sphingolipid <i>de novo</i> synthesis located in the ER.....	18
5. Different Ceramide synthases synthesize ceramides with different fatty acyl chain length..	19
6. Schematic representation of the pathways involved in ceramide metabolism with their subcellular localizations. ....	21
7. Pro-apoptotic vs. anti-apoptotic sphingolipids. ....	22
8. Structural analogy between fumonisin B1 and the sphingoid bases, sphinganine and sphingosine. ....	23
9. Mechanisms of action of functional inhibitors of ASM. ....	24
10. The expression level of p53 in HCT-116 p53 <sup>+/+</sup> and p53 <sup>-/-</sup> cells.....	40
11. Response of HCT-116 cells to hypoxia. ....	41
12. Ceramide accumulation upon hypoxia in HCT-116 p53 <sup>+/+</sup> and p53 <sup>-/-</sup> cells.....	43
13. Evaluation of the effect of GW4869 on the response of HCT-116 cells to hypoxia. ....	46
14. Evaluation of the effect of desipramine on the response of HCT-116 cells to hypoxia.....	47
15. Evaluation of the effect of fumonisin B1 or/and SK1-I on the response of HCT-116 cells to hypoxia. ....	51

16. Modulation of DEGS1 expression in response to hypoxia in both p53 <sup>+/+</sup> and p53 <sup>-/-</sup> HCT-116 cells.....	54
17. Ceramide and dihydroceramide species distribution in HCT-116 cells under physiological conditions. ....	55
18. Changes in the levels of medium and long chain ceramide species in HCT-116 cells subjected to hypoxia.. ....	57
19. Changes in the levels of very long and ultralong chain ceramide species upon hypoxia.....	58
20. Modulation of sphingosine kinase 1 (SphK1) mRNA expression and sphingosine levels in response to hypoxia in both p53 <sup>+/+</sup> and p53 <sup>-/-</sup> HCT-116 cells. ....	60
21. Evaluation of C6 ceramide impact on the response of HCT-116 cells to hypoxia...	62

## TABLES

Table	Page
1. Primer sequences of <i><math>\beta</math>-actin</i> , <i>DEGS1</i> and <i>SphK1</i> .....	37
2. List of primary antibodies.....	38

## ABBREVIATIONS

### A

A-CDase: Acid Ceramidase

APAF-1: Apoptotic protease-activating factor 1

APC: Adenomatous Polyposis Coli

A-SMase: Acidic Sphingomyelinase

ATP: Adenosine Triphosphate

ARC: Activity-regulated cytoskeleton-associated protein

### C

C1P: Ceramide-1-Phosphate

C1PP: C1P Phosphatase

CDK: Cyclin Dependent Kinase

CerS: Ceramide Synthase

CERT: Ceramide Transfer Protein

CIMP: CpG island methylator phenotype

CIN: Chromosome instability

CK: Ceramide Kinase

CRC: Colon or Colorectal Cancer

### D

DES: Dihydroceramide desaturase enzyme

*DEGS1*: Drosophila Degenerative Spermatocyte 1 gene

DGK: Diacylglycerol Kinase

DISC: Death-inducing-signaling-complex

DMEM: Dulbecco's Modified Eagle's Medium

## E

ECL: Enhanced Chemiluminescence

ER: Endoplasmic Reticulum

## F

FB1: Fumonisin B1

FBS: Fetal Bovine Serum

## G

GAPDH: Glyceraldehyde 3-Phosphate Dehydrogenase

GOF: Gain of function

## H

HCl: Hydrogen Chloride

HCT-116: Human Colorectal Carcinoma cell line

HIF: Hypoxia Inducible Factor

HRNP: Hypoxia-Responsive Nanoparticles

HRP: Horseradish Peroxidase



## K

KDS: 3-keto Dihydrosphingosine Reductase

## L

LC/MS: Liquid Chromatography–Mass Spectrometry

LOF: Loss of Function

## M

MAPK: Mitogen-Activated Protein Kinase

MDM2: Mouse Double Minute 2

MSI: Microsatellite Instability

## N

nSMase: Neutral Sphingomyelinase

## P

PARP: Poly (ADP-ribose) Polymerase

PBS: Phosphate Buffered Saline

PI: Propidium Iodide

pRb: Retinoblastoma Protein

PVDF: Polyvinylidene Difluoride

## R

rAd-p53: Recombinant Adenovirus - Wild-Type p53

RPMI: Roswell Park Memorial Institute Medium

## S

S1P: Sphingosine-1-Phosphate

SK1: Sphingosine kinase 1

SM: Sphingomyelin

SMases: Sphingomyelinases

SMSs: Sphingomyelin Synthase

*sphK1*: Sphingosine kinase 1

SK1-I: Sphingosine Kinase 1 Inhibitor

SPL: Sphingosine-1-Phosphate Lyase

SPT: Serine Palmitoyl Transferase

## T

TAA: Tumor-Associated Antigen

TBS: Tris Buffered Saline

TNF $\alpha$ : Tumor Necrosis Factor Alpha

## V

VHL: Von-Hippel-Lindau

## W

WT: Wild Type

# CHAPTER I

## INTRODUCTION

### *A. Colon Cancer*

#### *1. Epidemiology and risk factors*

Colon cancer, also known as colorectal cancer (CRC), is a disease characterized by the development of abnormal tumorous growths in the large intestine<sup>1</sup>. Colorectal cancer (CRC) is a common and fatal disease; it represents the third most common cause of cancer incidence<sup>2</sup>, and the fourth most deadly cancer in both men and women worldwide<sup>3</sup> with 1,849,518 new colorectal cancer cases (10.6% of all cancer incidents) and 880,792 deaths recorded in 2018. In Lebanon, 1,463 new colorectal cancer cases (regrouping colon, rectal and anal cancer episodes) were reported in 2018, accounting for 8.5% of all cancer events, with 851 cases of death from colorectal cancer declared<sup>4</sup>. Numerous environmental and genetic factors are known to increase the occurrence of colorectal cancer<sup>1,5</sup>.

Among colorectal cancer cases, 25% are accompanied with a family history of CRC, while over 60 % are sporadic, caused by somatic genetic and epigenetic defects, mainly referable to potentially modifiable risk factors<sup>6</sup>. Among these, aging is considered a major risk factor for colon cancer. Hence, CRC prevalence starts increasing significantly between the ages of 40 and 50<sup>5</sup>.

Environmental and lifestyle factors can also intervene in causing colon cancer. These include personal habits such as alcohol drinking, tobacco smoking, and sedentary lifestyle. For instance, being overweight or obese increases the risk of developing and dying from colorectal cancer<sup>7</sup>.

## ***2. Colon carcinogenesis and genetic basis***

The majority of colorectal cancer cases arise from a benign premalignant lesion so-called adenomatous polyp or adenoma<sup>8</sup>. However, a very minimal number of adenomas progresses into malignant lesions or carcinoma, which may invade surrounding tissues, and ultimately spread to other organs (metastasis)<sup>9,10</sup>. Sequential acquisition of genetic and epigenetic alterations in tumor suppressors or oncogenes drives the stepwise progression from adenoma to carcinoma<sup>10</sup>. In colon cancer, at least 3 distinct pathways of genomic instability have been described, the chromosomal instability (CIN), microsatellite instability (MSI), and the CpG island methylator phenotype (CIMP) pathways. The chromosomal instability (CIN) pathway, which underlies the majority of colon cancer cases, is characterized by the accumulation of numerical or structural chromosomal abnormalities, translated by a high rate of gains or losses of whole or large portions of chromosomes<sup>11</sup>. The typical karyotypic abnormalities resulting from the CIN pathway favor the onset of consecutive mutations mainly involving alterations in the Adenomatous Polyposis Coli (*APC*) gene, followed by oncogenic *KRAS* mutation and inactivation of the tumor-suppressor gene *TP53*<sup>12</sup> (Fig.1).

Mutations in the *TP53* gene tend to occur at the latest stage of colon carcinogenesis, conveying the colon cancer cells a greater potential of invasion and metastasis, as well

as one of the most important hallmarks of cancer, resistance to apoptosis. Cancer cells that acquire these mutations along with the emerging traits build up aggressive clones that overtake their wild-type counterparts, ultimately leading to a greater CRC progression and to poor prognosis<sup>12</sup>.

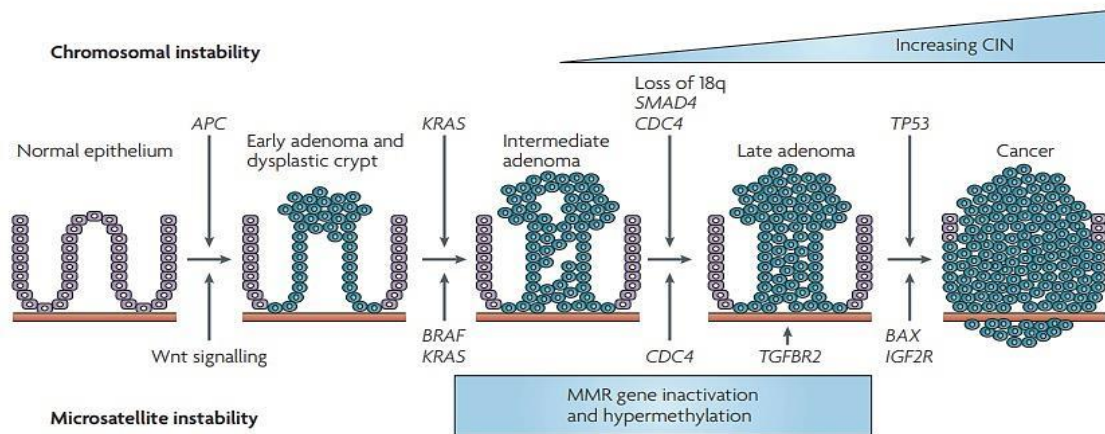


**Figure 1. Molecular events associated with CRC progression<sup>13</sup>.** The initial step in tumorigenesis, following the chromosomal instability (CIN pathway), is that of adenoma formation, associated with loss of *APC*. Larger adenomas and early carcinomas acquire mutations in the small GTPase *KRAS*, followed by loss of chromosome 18q with *SMAD4*, and mutations in *TP53* in frank carcinoma. Microsatellite instability (MSI) pathway is uncommon in adenoma, and it involves a different set of genetic alterations that affect Wnt signaling, *BRAF*, and other genes.

## B. *TP53* a tumor suppressor gene

### 1. Definition

*TP53* is the first tumor suppressor gene to be identified. Discovered over 40 years ago, p53 emerged as a key regulator of several oncogenes involved in growth and apoptosis such that, when this regulation is lost, cancer develops<sup>14</sup>. This gene is 20 kilobases (kb) long, located on the small arm of chromosome 17, and mapped to the chromosomal

region 17p13.1<sup>16</sup>. p53 protein is a DNA-binding transcription factor made up of a conserved proline rich domain preceded by two N-terminal transactivation domains, followed by a central DNA binding domain, and ending with a C-terminus encoding its nuclear localization signals and an oligomerization domain needed for its transcriptional activity<sup>17</sup>.

## ***2. p53 function***

The p53 protein has been designated as “the guardian of the genome” for its role in mediating the cellular response to DNA damage, preventing the emerging oncogenic mutations by killing the damaged cells, thus, maintaining genomic stability<sup>14,17</sup>.

Numerous studies have shown that p53 transcription factor targets many genes and microRNAs in response to cellular stress. p53 elicits its tumor-suppressor function through the transactivation of several genes implicated in the promotion of cell cycle arrest and/or apoptosis, in response to cellular stressors<sup>18</sup>.

Under normal conditions, p53 is bound to an E3 ubiquitin protein ligase MDM2, leading to its proteasomal degradation, and resulting in an extremely low baseline level of p53 expression<sup>19</sup>.

Upon stress circumstances such as DNA damage, ribonucleotide depletion, oncogenic activation, heat shock and hypoxia, p53 levels rapidly increase in the cell nucleus through post-translational modifications, which modulate its stability and activities, in order to bring into play p53 pro-apoptotic function. These chemical modifications, such as phosphorylation and acetylation, convert p53 from an inert to an active form, which might be due to the dissociation of MDM2 from p53<sup>19</sup>.

Depending on the severity and types of stress, functionally active p53 transactivates an appropriate set of its target genes including cell cycle checkpoints and/or apoptosis-inducing genes.

p53-mediated cell cycle arrest provides time for the cell to repair the genomic damage.

When DNA repair is complete, cells re-enter the normal cell cycle.

In contrast, when cells face severe DNA damage, p53 elicits its pro-apoptotic function to eliminate these cells and prevent the transfer of damaged DNA to daughter cells.

Thus, p53 has an ability to maintain genomic integrity<sup>20</sup>.

### **3. p53 and cell cycle**

As mentioned, following cellular stress such as DNA damage, and in order to provide time for the cell to repair the genomic damage before being released back into the proliferating pool, p53 induces cell cycle arrest<sup>21</sup>.

p53-mediated cell cycle arrest operates through the transcriptional activation of p21/WAF1<sup>22</sup>. p21 then leads to G<sub>1</sub> arrest by binding to and inhibiting cyclin E/CDK2 and cyclin D/CDK4 complexes. Inhibition of cyclin-CDK complexes results in the dephosphorylation and, thus, activation of the tumor suppressor retinoblastoma protein (pRb), stimulates pRb binding to E2F1, and promotes the transcription silencing of E2F1 targets critical for DNA replication and cell-cycle progression<sup>22,23</sup>.

p21 can also promote G<sub>2</sub>/M arrest and inhibit cyclin B/Cdc2 kinase activity, holding cell-cycle progression through mitosis<sup>22</sup>.

#### **4. p53 and apoptosis**

p53 is implicated in the induction of two different apoptotic signaling pathways: the intrinsic and the extrinsic pathways<sup>24</sup>. The extrinsic pathway requires the engagement of particular ‘death’ receptors that belong to the tumor necrosis factor receptor (TNF-R) family, and lead to a cascade of activation of caspases, including caspase-8 and caspase-3, through the formation of the death-inducing-signaling-complex (DISC), resulting in apoptosis<sup>20,25</sup>.

The intrinsic mitochondrial pathway can be induced following DNA damage. p53-mediated transactivation leads to apoptosis due to its ability to control transcription of proapoptotic members of the Bcl-2 family, such as the ‘multidomain’ Bcl-2 family member *Bax*, as well as the ‘BH3-only’ members *Puma*, *Noxa*, and *Bid* which leads to the release of cytochrome c from the mitochondria into the cytoplasm. Cytochrome c along with apoptotic protease-activating factor 1 (APAF-1) and procaspase-9 then form a complex termed the apoptosome, in which caspase-9 is activated and promotes activation of caspase-3, caspase-6 and caspase-7, inducing apoptosis<sup>25,26</sup>.

#### **5. p53 and cancer**

Recent advances in cancer research revealed that over 50% of human cancers including colon cancer are associated with mutations in the *TP53* gene<sup>20</sup>.

These mutations are typically ‘conformational p53 mutants’ which affect the structure folding, or the stability of the DNA-binding domain of p53. Some of p53 mutations designated as ‘contact site mutants’, inhibit the DNA binding, without altering the



structure of the DNA binding domain<sup>27</sup>. The loss of wild-type p53 function (LOF) as a DNA-binding transcription factor through the total lack of p53 expression, or the production of unstable or truncated mutant proteins, disfavors the p53-mediated tumor-suppressive responses, ultimately leading to cancer development<sup>28</sup>.

Beside wild-type p53 loss of function, a subset of p53 missense mutations generates full length protein with a single amino acid substitution, conferring p53 pro-tumor traits<sup>27</sup>. In this case, the gain of function (GOF) of mutant p53 supports cancer cell survival, tumor progression, invasion, metastasis and chemoresistance<sup>28</sup>. Cellular stressors, such as radiation therapy, chemotherapy, and hypoxia, subsequently act as environmental selectors for the robust clones, such that the population harboring the neomorphic p53 mutation tends to overtake the wild-type clones, thereby accentuating tumor aggressiveness.

Nevertheless, the timing of occurrence of *TP53* mutations during cancer progression may vary from one cancer type to another; for instance, in colon cancer, these mutations preferentially occur relatively at a late stage during the transition from late adenoma to carcinoma<sup>29</sup>.

## **6. Targeting p53**

Several therapeutic strategies targeting the mutant form of p53 were proposed. These strategies aim to restore the wild-type p53 function and prevent cancer progression.

The adenoviral delivery of wild-type p53: cancer cells are transduced using a recombinant adenovirus engineered to express wild-type p53 (rAd-p53). Depending on cellular stress conditions, WT p53 mediates cell-cycle arrest and DNA repair, or

induces apoptosis, senescence, and/or autophagy, therefore controlling cancer progression. However, host antibodies produced in response to the adenoviral infection reduce adenovirus infectivity and dampen the introduction of p53 wild-type form, which largely alters the efficacy of this approach<sup>30</sup>.

Inhibition of p53-MDM2 interaction: MDM2 is an E3 ubiquitin ligase that inhibits p53 transcriptional activity, favors its nuclear export, and drives its proteasomal degradation. The inhibition of p53-MDM2 interaction with synthetic molecules should therefore lead to p53 nuclear accumulation and its activation, followed by tumor cell death. This strategy targeting wild-type p53-expressing clones, ultimately leads to the undesirable side effect of p53 accumulation in normal cells, engendering apoptosis in highly proliferating tissues such as the hematopoietic system and the intestinal epithelium<sup>31,32</sup>.

Restoration of mutant p53 to wild-type p53: knowing that *TP53* is mutated in the majority of cancer types, studies on mouse models of human lymphoma and sarcoma, and on murine liver carcinoma suggested that restoring p53 function can inhibit cell proliferation, induce cellular senescence, and result in tumor regression<sup>33,34</sup>.

Nevertheless, sustained wild-type p53 restoration has been shown to drive the emergence of resistant clones through the inactivation of p19 (ARF) which initially attenuates MDM2-mediated degradation of p53<sup>32,36</sup>.

p53-based vaccines: when p53 undergoes a point mutation, its half-life is extended leading to its accumulation in the tumor tissue. In this case, mutated p53 is considered as a tumor-associated antigen (TAA) that can be recognized by T lymphocytes and induce their activation. Several immunization clinical trials were conducted using different strategies for p53-based vaccines ranging from viral vectors, dendritic cells, to

short and long peptides. Despite the p53-specific response that was induced, robust clinical responses were not achieved<sup>36</sup>.

In conclusion, strategies aiming to reimpose WTP53 expression and function, despite their promise, were faced with several limitations translated by a poor clinical response. This might be due to the emergence of different p53-mutants along with variable resistance strategies. Exploring alternative mechanisms able to restore the pro-apoptotic function that is lost with p53 mutation could potentially restore tumor regression.

## **C. Solid tumors and hypoxia**

### ***1. Solid tumors***

A solid tumor is a benign or malignant mass of tissue that usually does not contain cysts or liquid<sup>37</sup>. As cancer cells grow, they diverge from normalcy and become increasingly resistant compared to the surrounding normal tissue. The 3D expansion of tumors ends by the development of clones far from the vessels which provide cells with metabolic requirements<sup>40,41</sup>. The heterogeneity in solid tumors occurs as the tumor mass enlarges with insufficient neovascularization resulting in a decreased supply of oxygen that gives rise to hypoxic regions within these tumors<sup>41</sup>.

### ***2. Vasculature***

Angiogenesis is defined as the biological process in which new blood vessels are formed from pre-existing vessels<sup>42</sup>. The transition from the avascular to the vascular phase is a critical turning point in solid tumor growth<sup>42,43</sup>. In order to support the high

proliferative rate of cancer cells that are prone to deficit in oxygen and nutrient levels, tumors release pro-angiogenic factors aiming at the development a new vascular network<sup>42</sup>. On the other side, healthy cells, having enough nutrients and oxygen, release anti-angiogenic factors. The conflict (imbalance) in the production of pro and anti-angiogenic factors enhances the formation of blood vessels with atypical morphological features compared to normal tissues vasculature<sup>42,44</sup>.

In general, the tumor vascular network is characterized by immature, tortuous and disorganized blood vessels knowing that the vascular immaturity results in excessive permeability and poor perfusion, therefore leading to a high degree of vascular heterogeneity<sup>44</sup>, with hyper vascular sites and other regions of low vessel density, so-called hypoxic regions<sup>45</sup>.

### **3. Hypoxia**

Hypoxia is a common feature for locally advanced solid tumors, caused by inadequate oxygen delivery through the abnormal vasculature that fails in supporting rapidly proliferating cancer cells<sup>45</sup>.

As a result, hypoxia is characterized by an oxygen tension  $\leq 2\%$ , lower than the physiological levels that are supplied to mammalian tissues, which range between 2 and 9%. Severe hypoxia or “anoxia” is reached when oxygen levels are below 0.02%<sup>46</sup>.

The reaction of cancer cells to the reduced oxygen tension depends on the duration and severity of hypoxic exposure<sup>47</sup>. During mild hypoxic conditions, cell-survival pathways are triggered, unnecessary growth is inhibited, and cellular metabolism is altered<sup>48</sup>.

These pro-survival functions are mainly orchestrated by a family of ubiquitous transcription factors known as hypoxia inducible factors (HIFs).

However when cells undergo a stressful prolonged hypoxia, DNA breaks and DNA replication errors occur, potentially leading to genetic instability and mutagenesis<sup>47</sup>. This therefore activates p53 transcription factor which allows time for the DNA repair machineries to restore genome stability by halting the cell cycle progression. If the damage is too severe to repair, p53 drives cancer cells to undergo apoptosis to prevent the propagation of DNA damage to daughter cells<sup>49</sup>.

#### ***4. Hypoxia Inducible Factors (HIFs)***

##### **a. Definition**

HIF is a transcription factor known to orchestrate the cellular response to hypoxia<sup>50</sup>. When oxygen is scarce, HIF activates genes involved in oxygen consumption, erythrocyte production, angiogenesis, and mitochondrial metabolism<sup>51</sup>.

It also allows cells to adapt to hypoxic stress by reducing oxygen consumption through a shift to glycolysis rather than oxidative metabolism, and by lowering energy demand for different cellular processes such as cell division<sup>51,52</sup>.

##### **b. Structure of HIF-1**

HIF exists in three different isoforms: HIF-1, HIF-2, and HIF-3. HIF-1, the most studied isoform, is recognized in tumor environment and considered as a key regulator of tumor progression<sup>52</sup>. HIF-1 is a heterodimer, made up of two subunits: the cytoplasmic oxygen-dependent  $\alpha$ -subunit, and the constitutively expressed nuclear  $\beta$ -subunit<sup>50,53</sup>.

- i. Under normal oxygen tension: HIF-1 $\alpha$  is hydroxylated by prolyl hydroxylases (PHDs). The hydroxylated HIF-1 $\alpha$  binds to Von Hippel Lindau protein (VHL) which is an onco-suppressor protein in the cytoplasm, resulting in HIF-1 $\alpha$  proteasomal degradation<sup>50</sup> (Fig.2).
- ii. Under hypoxic conditions: prolyl hydroxylase enzyme is inactive and HIF-1 $\alpha$  is stabilized and translocated to the nucleus, where it dimerizes with HIF-1 $\beta$ , and together they form the HIF-1 complex. This complex binds to DNA and acts as a transcription factor involved in angiogenesis, and the modulation of cellular metabolism in order to overcome hypoxia<sup>50,51</sup> (Fig.2).

#### ***5. Cross-talk between HIF-1 and p53 under hypoxic conditions***

Oxygen sensing and reactivity to changes in the concentration of oxygen is a fundamental property of cell physiology. Under severe hypoxic conditions for prolonged incubation periods, HIF suppresses MDM2-mediated p53 proteasomal degradation leading to p53 stabilization<sup>54,55</sup>.

Under anoxia, the high levels of p53 trans-repress HIF-1 $\alpha$ , and engender canonical tumor-suppressive pro-apoptotic activities<sup>54,56</sup>(Fig.2).

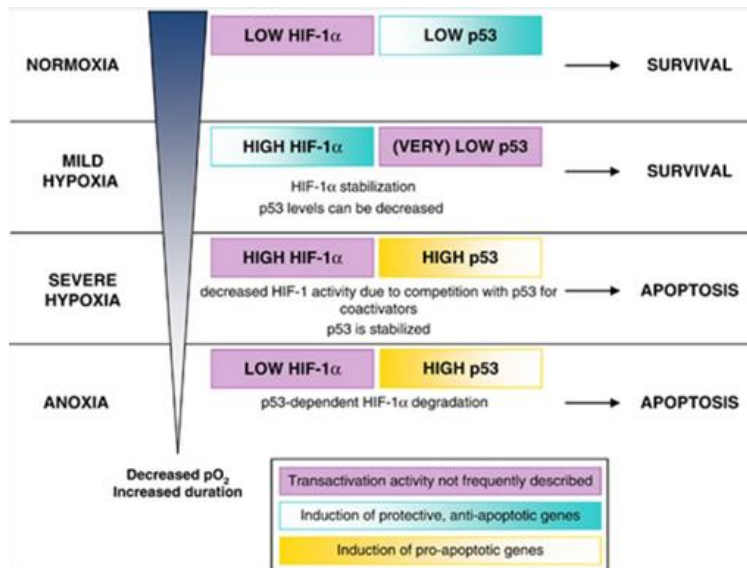


**Figure 2. Regulation of p53 and HIF pathways depending on the severity and duration of hypoxia.** Under normoxia or mild hypoxia, HIF-1 $\alpha$  is stabilized and p53 protein level is decreased, therefore, promoting survival. Severe hypoxic conditions induce p53 which competes with HIF-1 $\alpha$  for the recruitment of coactivators, hence, decreasing HIF-1 $\alpha$  activity and promoting apoptosis. Under anoxia, p53 protein level increases further inducing HIF-1 $\alpha$  degradation and subsequent apoptosis<sup>54</sup>.

## 6. Hypoxia inducible p53 mutation

In order to evade hypoxia-induced p53-mediated cell death and growth arrest, cancer cells that develop favorable mutations of the *TP53* tumor-suppressor gene become selected and are preferentially propagated. Unlike WTp53, mutant p53 coordinates adaptive responses to the hypoxic stress occurring in solid tumors in a way that supports their progression and resistance. Hypoxia then acts as a potent selector for the robust mutp53 clones and leads to their expansion at the expense of their WT counterparts<sup>28</sup>.

The hypoxia-dependent clonal selection and expansion of mutant clones is likely mediated by the transcription factor heat-shock factor-1 (HSF1), which, under stress, is activated and induces high Hsp90, a chaperon protein that binds to mutp53 and inhibits its degradation by MDM2. These changes result in clonal expansion of cells harboring the tumor-promoting mutant p53, thereby accentuating tumor aggressiveness<sup>28,56</sup>.

### ***7. Targeting p53 mutation under hypoxic conditions***

Since the loss of the pro-apoptotic function of p53 is pervasive in hypoxic areas of solid tumors, the therapeutic targeting of p53 mutation under hypoxic conditions has garnered significant research interest. One of the main strategies that was previously proposed aimed at the restoration of WTp53 conformation following the re-oxygenation of MCF-7 and HCT-116 xenografts<sup>57</sup>. Although this strategy was promising at first glance, however hyperoxia was demonstrated to generate reactive oxygen species which eventually provoked tissue injury.

An alternative approach aimed at targeting the homeodomain-interacting protein kinase-2 (HIPK2). HIPK2 typically activates p53 by phosphorylating it at serine 46, leading to apoptosis; additionally, it suppresses hypoxia inducible factor 1 $\alpha$  (HIF-1 $\alpha$ ), a key player in angiogenesis and metastasis discussed earlier. When oxygen is scarce, HIPK2 is down-regulated. Although zinc supplementation restores the function of HIPK2, and hence p53-triggered apoptosis, this approach may reactivate the mutant p53 and exacerbate conditions<sup>58,59</sup>.

Altogether, these findings demonstrate the failure of several different approaches to restore p53 function inside a heterogeneously-oxygenated tumor microenvironment



harboring different p53-mutant forms. Hence, finding an alternative approach able to mimic p53 function and to work independently of its status is worthy of consideration.

#### **D. Ceramide, a bioactive sphingolipid**

##### ***1. Chemical structure of ceramide***

Ceramide is the neutral lipid building block of sphingolipids, made up of sphingosine, an 18-carbon amino alcohol hydrocarbon chain, which is joined *via* an amide bond to a fatty acid<sup>60,61</sup>. The fatty acyl component of ceramide may vary widely in composition, in length (ranging from 14 to above 26 carbon atoms) as well as in saturation (saturated or unsaturated), which results in many ceramide species and dictates their biological activities<sup>61-63</sup> (Fig.3).

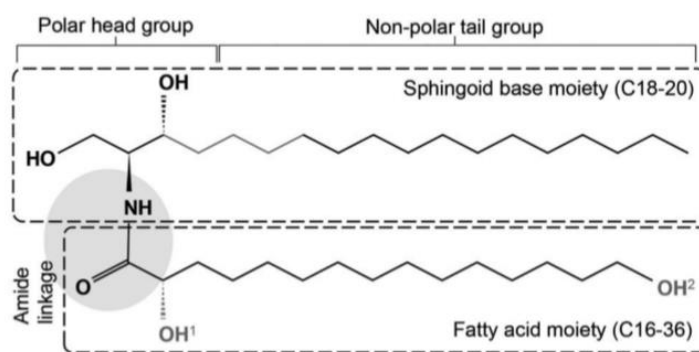


**Figure 3. Chemical structure of ceramide.** Ceramide is composed of a sphingoid base, sphingosine, bonded by an amide linkage (in grey) to a fatty acyl chain. The sphingosine contains a polar head group and a non-polar tail group.

## 2. *Bioactive role of ceramide*

Sphingolipids, beside the structural role they play in bio-membranes, are also involved in signal transduction and cell function regulation<sup>64</sup>.

As a bioactive sphingolipid, ceramide has been implicated in mediating or regulating a variety of physiological functions including apoptosis, cell cycle arrest, differentiation, cell senescence, cell migration and adhesion<sup>64</sup>. Ceramide and its metabolites have been extensively investigated in a number of pathophysiological conditions including cancer, neurodegeneration, diabetes, microbial pathogenesis, and cardiac diseases<sup>65</sup>.

## 3. *Ceramide synthesis*

Depending on the cell type and stimulus, ceramide is generated by three major pathways: the *de novo* synthesis, the salvage and the sphingomyelinase pathways.

a. The *de novo* synthesis pathway

The *de novo* synthesis of ceramide commences in the endoplasmic reticulum (ER) by the condensation of L-serine and palmitoyl-CoA by the serine palmitoyl transferases (SPT), generating 3-ketosphinganine<sup>63</sup>. 3-Ketosphinganine is subsequently reduced to sphinganine in a reaction catalyzed by 3-ketosphinganine reductase (KDSR).

Sphinganine is then N-acylated by ceramide synthases (CerS), thereby forming dihydroceramides<sup>66,67</sup>. Dihydroceramide is subsequently desaturated by a dihydroceramide desaturase (DEGS), resulting in ceramide production<sup>68</sup> (Fig.4). The desaturation of dihydroceramide to ceramide requires the introduction of a *trans* double bond between carbons C-4 and C-5. This double bond is largely responsible for ceramide biological activity including the regulation of cell growth, arrest, survival and death.

The formed ceramides (Cer) are subsequently shuttled to the Golgi apparatus either through the ceramide transfer protein CERT or by vesicular transport<sup>69</sup>. In the Golgi, ceramide gives rise to complex sphingolipids such as glycosphingolipids and sphingomyelin (SM)<sup>70</sup>. Afterwards, sphingomyelin and glycosphingolipids are transported to the plasma membrane through vesicular flow<sup>71</sup>.

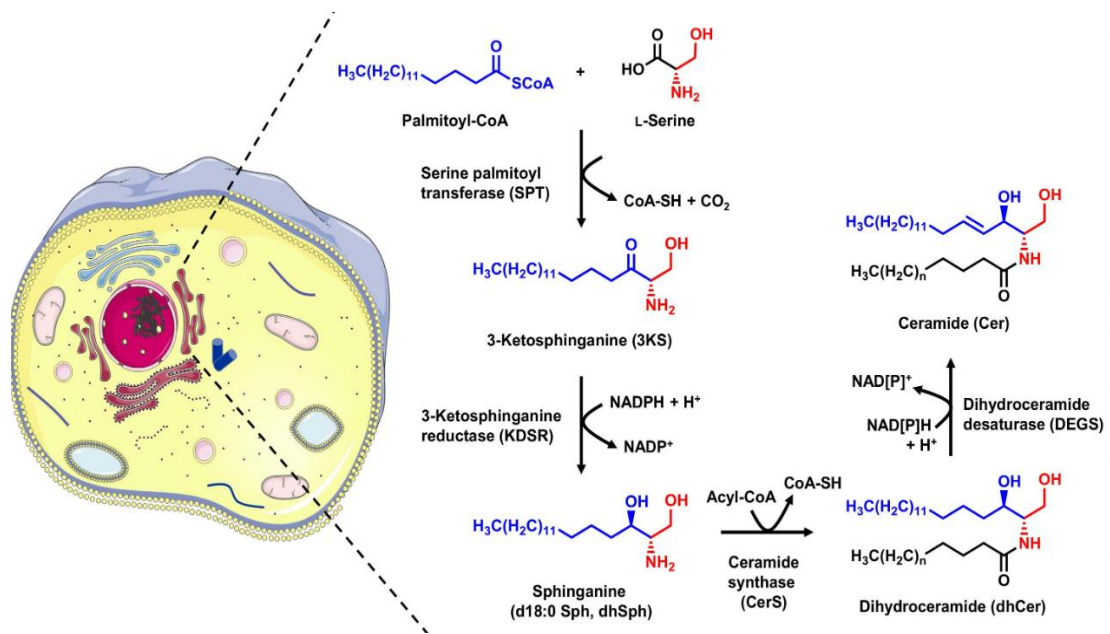


**Figure 4.** Schematic overview of the sphingolipid *de novo* synthesis located in the ER.

i. Ceramide synthases (CerSs)

Ceramide synthases (CerSs) are the enzymes in charge of ceramide production from sphingoid bases and acyl-CoA substrates<sup>72</sup>. These enzymes regulate simultaneously the *de novo*, as well as the salvage pathway of ceramide synthesis, which will be discussed later on. Six mammalian CerSs (CerS1–CerS6) have been identified to date. Despite displaying common characteristics such as their structure, intracellular localization, as well as their reactional mechanism, each of the CerSs preferentially uses fatty acyl-CoAs of defined chain length for ceramide synthesis<sup>73</sup> (Fig.5).

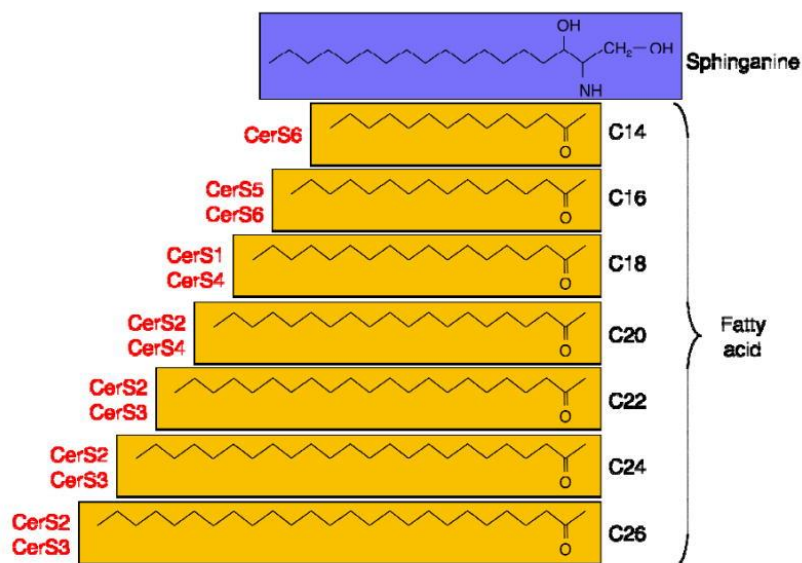


**Figure 5. Different Ceramide synthases synthesize ceramides with different fatty acyl chain length.** Ceramides can differ in their fatty acyl chain length as well as their degree of saturation. Sphinganine is shown in blue, the fatty acyl chain in yellow, and the CerS that synthesizes each type of ceramide is shown in red<sup>74</sup>.

ii. Dihydroceramide desaturase (DEGS)

Dihydroceramide desaturase is the last enzyme in the *de novo* synthesis of ceramides. It inserts a double bond between carbons 4 and 5 of the sphinganine base of dihydroceramides, catalyzing their conversion into ceramides<sup>75,76</sup>.

Two different dihydroceramide desaturases (DEGS1 and DEGS2) have been identified. They differ in their tissue distribution, with DEGS1 being ubiquitously expressed, while DEGS2 expression is restricted to skin, intestine and kidney<sup>76</sup>.

b. Sphingomyelin hydrolysis

Sphingomyelin (SM) is the most abundant complex sphingolipid in mammals, and its coordinated breakdown plays an essential role in membrane homeostasis<sup>77</sup>. Breakdown

of sphingomyelin occurs either in the plasma membrane or in the acidic compartment, the endolysosome<sup>66</sup>. Sphingomyelin hydrolysis is catalyzed by sphingomyelinases (SMases), and results in the production of ceramide and free phosphocholine<sup>77,78</sup>.

Based on the pH required for their optimal activity, sphingomyelinases fall into three major categories: acid, alkaline, and the neutral sphingomyelinases. All sphingomyelinases isoforms catalyze a similar reaction; however they differ in their organ localization and subcellular distribution<sup>77</sup>.

Alkaline sphingomyelinase is mostly expressed in the intestine and liver and plays a role in the digestion of dietary sphingomyelin. Acid and neutral sphingomyelinases are expressed ubiquitously and they regulate sphingomyelin catabolism in most tissues<sup>66,77</sup>.

Neutral sphingomyelinases are responsible for the plasma membrane sphingomyelin hydrolysis, whereas A-SMase hydrolyze the endo-lysosomal sphingomyelin, taking part of the salvage pathway.

### c. Salvage pathway

The recycling of free sphingosine produced via ceramidases from the breakdown of pre-formed complex sphingolipids such as complex glycolipids is termed the 'salvage pathway'<sup>79,80</sup>. This pathway occurs in acidic cellular compartments such as lysosomes and late endosomes, contributing to 50-90% of the sphingolipid biosynthesis<sup>67</sup>.

Sphingosine can be generated through sphingomyelin hydrolysis catalyzed by the A-SMase, or through the breakdown of complex sphingolipids such as glycosphingolipids. Such degradation results from the cleavage of sugar residues, leading to the formation of glucosyl and galactosyl ceramide, which can then be hydrolyzed by specific  $\beta$ -glucosidase and galactosidase resulting in the generation of ceramide. Ceramidases can

further convert the produced ceramide into sphingosine<sup>81</sup> which can be released from the lysosome into the ER where it can be recycled back into ceramide by CerSs<sup>82,83,67,78</sup> (Fig.6).

Alternatively, sphingosine can be phosphorylated by sphingosine kinases leading to the

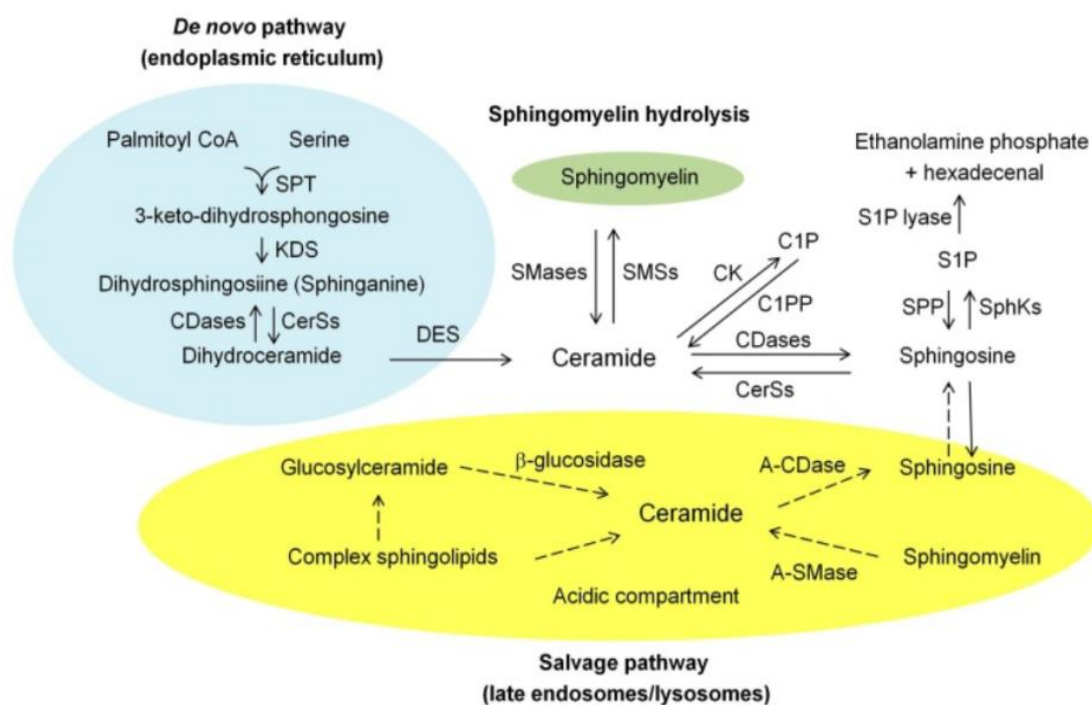


**Figure 6. Schematic representation of the pathways involved in ceramide metabolism with their subcellular localizations.** Ceramide can be generated via three major pathways: (1) The *de novo* pathway which occurs in the endoplasmic reticulum (ER), (2) The hydrolysis of sphingomyelin (SM) which takes place in the plasma membrane, (3) The salvage pathway which occurs in acidic cellular compartments (lysosomes and late endosomes). A-CDase, acid ceramidase; A-SMase, acidic sphingomyelinase; CerSs, ceramide synthases; KDS, 3-keto dihydrospingosine reductase; CK, ceramide kinase; C1P, ceramide-1-phosphate; C1PP, C1P phosphatase; DES, dihydroceramide desaturase; SMases, sphingomyelinases; SMSs, sphingomyelin synthases; SphKs, sphingosine kinases; S1P, sphingosine-1-phosphate; SPP, S1P phosphatase; SPT, serine palmitoyl transferase.

production of S1P, that can be either recycled back into sphingosine by specific phosphatases, or alternatively, can be irreversibly degraded by S1P lyase (SPL)<sup>84,85</sup>. Likewise, ceramide may also be reversibly phosphorylated by ceramide kinase<sup>84</sup> into C1P. Unlike ceramide and sphingosine, which generally mediate cell death and growth arrest, S1P and C1P act as growth promoting, anti-apoptotic molecules<sup>85</sup> (Fig.7).

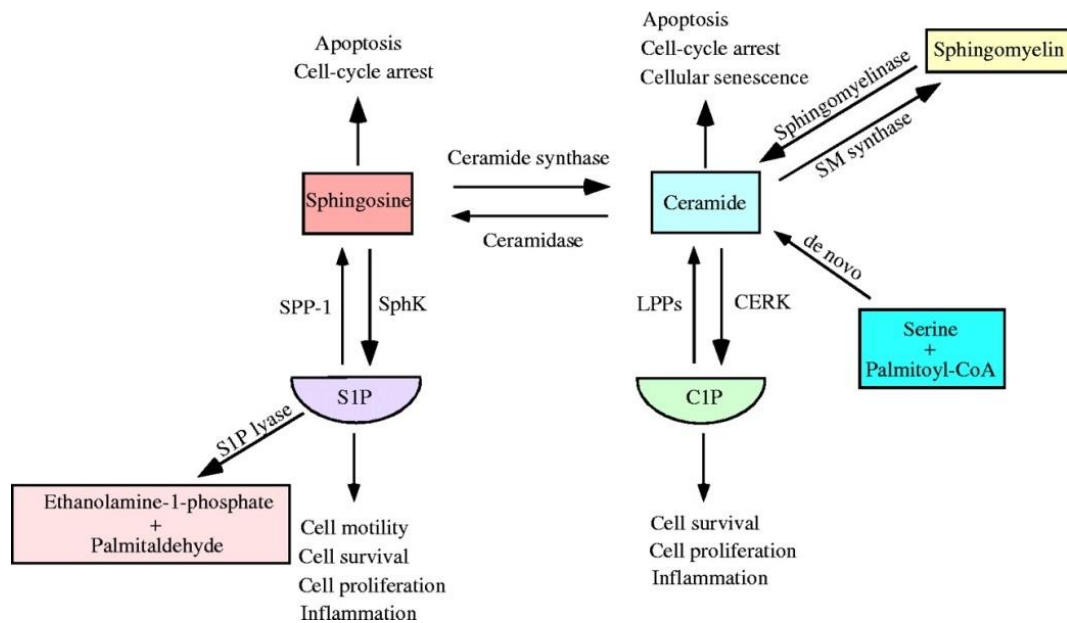


**Figure 7. Pro-apoptotic versus anti-apoptotic sphingolipids.** Ceramide and sphingosine act as pro-apoptotic lipids, C1P and S1P are considered as oncometabolites, and dihydroceramide (DHCer) is generally believed to be biologically inert.

### E. Inhibitors of ceramide metabolism enzymes



## 1. Fumonisin B1

Fumonisin B1 (FB1) is a mycotoxin that inhibits CerSs. Owing to its remarkable structural analogy with the sphingoid bases sphinganine and sphingosine (Fig.8), FB1 acts as a competitive inhibitor that occupies the place of these substrates in CerS enzyme<sup>86,87</sup>. CerS inhibition by FB1 not only blocks ceramide synthesis, but also triggers a cascade of perturbations in ceramide metabolites including dihydroceramides, sphinganine, sphingosine and their phosphorylated forms, glycosylated ceramides and other complex sphingolipids<sup>88</sup>.

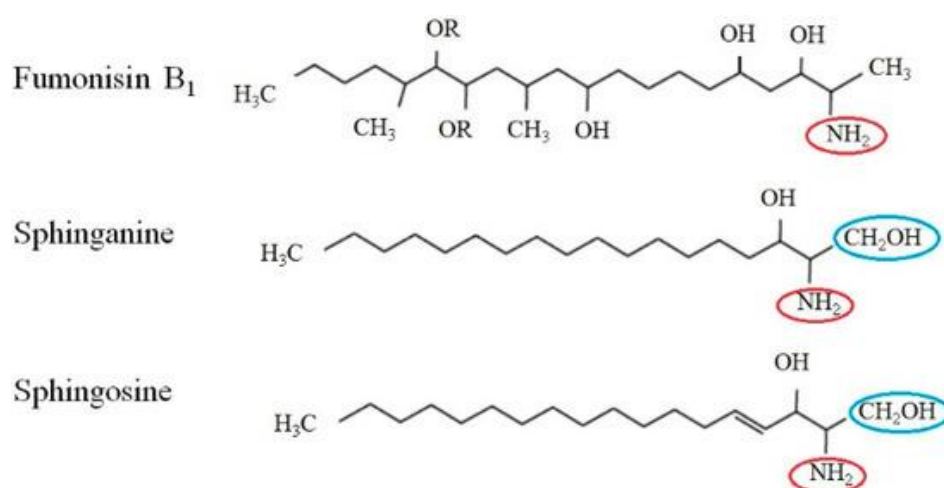


**Figure 8. Structural analogy between fumonisin B1 and the sphingoid bases, sphinganine and sphingosine.** The chemical structure of FB1 is similar to that of sphinganine and sphingosine, all having an amine group (red circle) attached to the long fatty-acid chain. FB1 also differs from sphinganine and sphingosine by the absence of a hydroxymethyl group (blue circle) attached to the head group.

## 2. Desipramine

Desipramine is a tricyclic antidepressant that belongs to the family of the functional inhibitors of acid sphingomyelinase (FIASMA). These inhibitors enter into the inner leaf of the lysosomal membrane and cause the detachment of the membrane-associated enzymes. Once detached from the membrane, ASMases will be cleaved and degraded in the lysosome<sup>89</sup>(Fig.9). Inhibition of ASMases by desipramine blocks the synthesis of ceramide through the salvage pathway, and affects other metabolites such as sphingosine and SIP<sup>90</sup> (Fig.9).

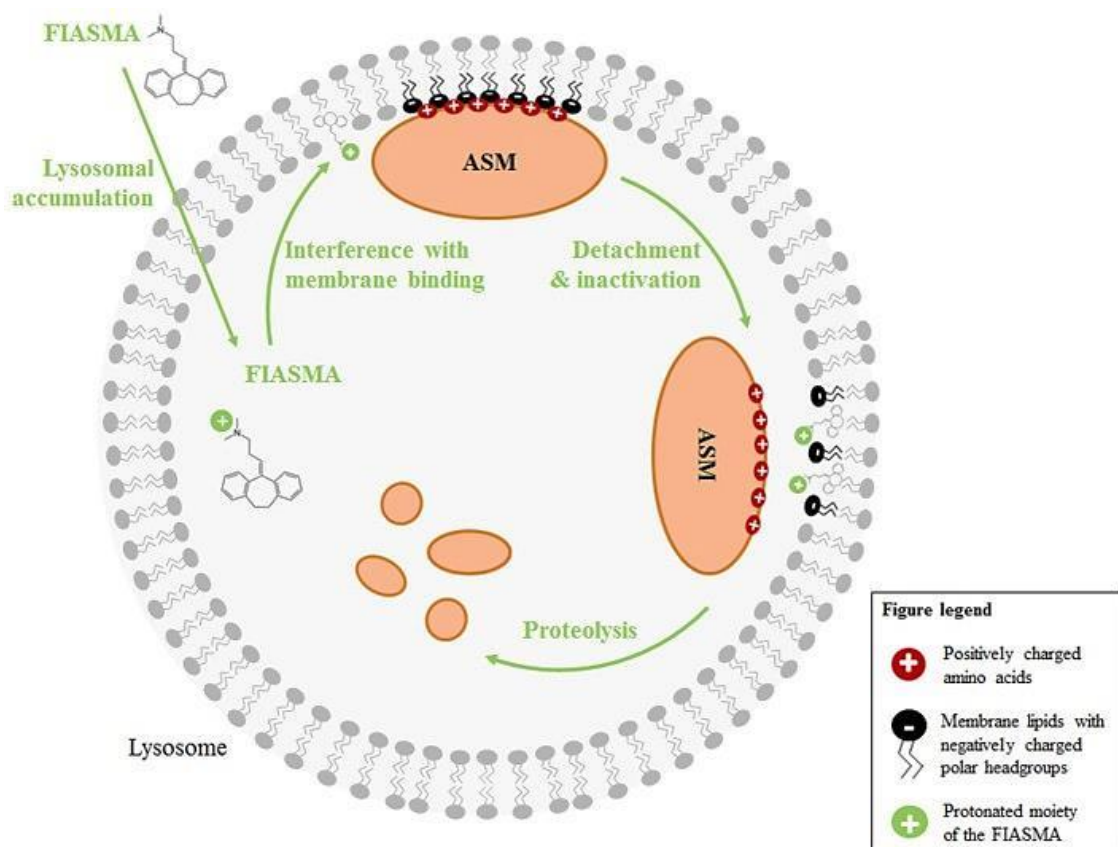


**Figure 9. Mechanisms of action of functional inhibitors of ASM.** FIASMA are weak bases that accumulate in acidic compartments like the lysosome. As a result, the electrostatic adherence of ASM to the membrane is lost and A-SMase are degraded<sup>90</sup>.

### **3. *GW 4869***

GW 4869 is a selective inhibitor of neutral sphingomyelinases (nSMase), frequently used in studying nSMase function in different cellular and animal models<sup>91</sup>.

GW4869 does not compete with the substrate sphingomyelin; however, this pharmacological inhibitor is competitive with phosphatidylserine that is essential for the activation of neutral sphingomyelinase when bound<sup>92</sup>.

### **4. *Sphingosine kinase 1 inhibitor SK1-I***

SK1-I is a selective inhibitor for sphingosine kinase 1. The structure of this inhibitor resembles that of sphingosine; therefore, it acts by competing with sphingosine in the sphingosine kinase binding site. This inhibitor blocks the phosphorylation of sphingosine into S1P, resulting in the decrease of S1P and the accumulation of sphingosine<sup>93,94</sup>.

#### **A. *Ceramide***

##### **1. *Ceramide structure-function relationship***

As described in the previous section, the structural and functional heterogeneity of different ceramide species underlines the importance of CerSs, which generate specific ceramides with distinct fatty acyl chain length. In fact, slight changes in the molecular structure of ceramide can regulate its biological function<sup>95</sup>.

For example, CerS1 specifically generates ceramides with an 18-carbon fatty-acid chain (C18 ceramide) having a pro-apoptotic role in neck squamous cell carcinomas, whereas CerS5–6 mainly generate C16-ceramide<sup>97,98</sup>, having pro-survival role in human head squamous cell carcinomas<sup>95,97</sup>. Moreover, C16 and C24-ceramide levels were particularly elevated in breast cancer tissue when compared to non-tumoral tissue, with C16 ceramide being correlated with metastasis to lymph nodes<sup>98</sup>. In addition, dihydroceramide, which differs from ceramide only by the reduction of the C4–5 *trans*-double bond in the sphingoid backbone, loses by this reaction its apoptotic signature<sup>60,99</sup>.

## ***2. Ceramide: an anti-cancer target***

As previously mentioned, ceramide was conventionally classified as a ‘ tumor suppressor lipid ’, since it effectively enhances signaling events that lead to apoptosis, cell cycle arrest, and autophagic responses<sup>80</sup>. Previous studies have demonstrated that traditional anti-cancer approaches trigger cell death through endogenous ceramide accumulation. These approaches include radiotherapy, and chemotherapies such as etoposide, daunorubicin, camptothecin, fludarabine, cisplatin and gemcitabine<sup>61,100</sup>. However, an overexpression of the ceramide-metabolizing enzymes enhances the production of other ceramide metabolites, which generally promote cell survival and ultimately cause the resistance to conventional therapies<sup>84,101</sup>. Therefore, targeting ceramide-metabolizing enzymes through specific inhibitors has been investigated. For instance, an acid ceramidase (A-CDase) inhibitor, DM102, prevents ceramide hydrolysis and sensitizes prostate cancer cells to cytotoxic agents

such as 4-HPR<sup>102</sup>. Likewise, sphingosine kinase inhibitors, which target the ceramide/S1P axis, have shown an anti-tumor activity against different types of cancer including leukemia, glioblastoma, neuroblastoma and multidrug-resistant tumor cells<sup>103</sup>. Moreover, the modulation of endogenous ceramide levels through the administration of short chain cell permeable ceramide analogs (C2, C6 and C8 Cer) has been extensively studied. Despite the promise of this strategy *in vitro*, several challenges arise *in vivo* and require the enhancement of the biophysical and chemical properties of ceramide analogs in order to improve their solubility and bioavailability inside the tumors<sup>104</sup>.

### **3. Ceramide and apoptosis**

As an active signaling lipid, ceramide influences diverse cellular physiological and pathophysiological processes such as programmed cell death. In fact, ceramide can induce apoptosis by modulating the activities of protein phosphatases such as PP1 and PP2A after binding to C1B lipid binding domain, resulting in BAX de-phosphorylation and activation of its pro-apoptotic function<sup>65</sup>.

Moreover, ceramide can directly bind to the aspartic protease, cathepsin-D (associated with TNF- $\alpha$ , Fas and chemotherapy-induced apoptosis) leading to autolytic cleavage of the pro-enzyme and resulting in its proteolytic activation in the lysosome. This ceramide-induced cathepsin D activation mediates cleavage and subsequent activation of the pro-apoptotic Bcl-2 family member Bid in response to TNF- $\alpha$ <sup>105</sup>.

### **4. Ceramide and p53**

Both p53 and ceramide have been involved in the modulation of growth suppression in response to cellular stress<sup>67</sup>. Understanding the connection between these two molecules and defining the molecular order that correlates both stress-induced pathways helps elucidating the mechanism of their action.

Following DNA damage, both p53-dependent and p53-independent stress response pathways could be activated. Ceramide can function independently of p53, downstream or, under unique circumstances, upstream of p53 activation<sup>97,106</sup>.

a. Ceramide downstream of p53

Studies have shown that exposing MOLT-4 leukemia cells to actinomycin D and  $\gamma$ -irradiations induced p53-dependent ceramide accumulation and apoptosis. MOLT-4 cells lacking p53 were resistant to  $\gamma$ -irradiation and did not accumulate ceramide<sup>107</sup>. The p53 up-regulation was followed with *de novo* ceramide synthesis preceding the apoptotic phenotype observed. Moreover, treating p53-deficient leukemia cells with exogenous cell-permeable ceramide analogues induced apoptosis independently of p53.

Similarly, when treating colon cancer cells (EB-1) with ZnCl<sub>2</sub>, p53 expression was increased engendering an elevation in ceramide levels. In contrast, colon cancer cells lacking p53 (EB), did not register any increase in ceramide levels upon treatment<sup>108</sup>.

Together these results confirm that p53 functions upstream of ceramide in response to genotoxic stress.

b. Ceramide upstream of p53

A study published by Pruschy *et al.*, reported that treatment of mouse fibrosarcoma cells with neutral sphingomyelinase drastically reduced cell proliferation in the presence of p53. In contrast, this effect was not observed in tumor cells lacking p53<sup>106</sup>. Similarly, C2 ceramide was able to induce apoptosis in p53-proficient but not in p53-deficient mouse fibrosarcoma cells. Since ceramide pathways evolved at a much earlier stage than p53, e.g. they are present in yeast whereas p53 is not, it is highly unlikely that ceramide is dependent on p53 for its activities as the authors concluded but their observations may have been system-specific as they were not replicated elsewhere<sup>106</sup>.

c. Ceramide and p53 independent pathways

In other studies, p53 and ceramide were placed in two independent pathways as ceramide has been shown to induce apoptosis irrespective of p53 status. Dbaibo *et al.*, for instance have demonstrated a p53-independent ceramide accumulation as a result of growth suppression induced by TNF- $\alpha$ , indicating that the connection between ceramide and p53 is only limited to certain stimuli such as genotoxic stress<sup>67,109</sup>.

In addition, Tamoxifen treatment was shown to induce ceramide-mediated apoptosis regardless of p53 status in colorectal cancer cells HCT-15, HT-29 and LOVO<sup>97</sup>.

In conclusion, the preponderance of data suggests that ceramide is the more primitive stress response, especially in the context of DNA damage and cancer, and that p53 evolved at a later stage and partially engaged the ceramide pathways. Therefore, the manifestations of this interplay between p53 and ceramide are complex and may vary depending on the cell type and stimulus but indicate that p53 is generally upstream of ceramide. This makes ceramide pathways functioning downstream of p53 attractive candidates for modulation when p53 is mutated, deleted, or otherwise disabled.

### 5. *Ceramide: mediator of the cellular response to hypoxia*

Besides their function as building blocks of sphingolipids, ceramides were found to be involved as signaling molecules in several biological processes, such as inflammation, cellular differentiation, and cellular stress responses<sup>110</sup>. For example, after exposure to hypoxia, total cellular ceramide concentration increases, and can in turn drive cell death pathways<sup>111</sup>. As previously mentioned, the cellular adaptation to hypoxia is predominantly mediated by hypoxia-inducible factors (HIFs)<sup>112</sup>. However, HIF-independent responses to hypoxia have been extensively studied in different cellular and animal models. These responses can be orchestrated by p53 or by different metabolic pathways such as the ceramide metabolism<sup>113</sup>.

We have previously shown that DEGS1, which catalyzes the final step of *de novo* ceramide biosynthesis, by inserting a *trans* double bond across carbons 4 and 5 of dihydroceramide converting it to ceramide, acts as a checkpoint in the regulation of ceramide-based responses to hypoxia. We demonstrated, in a hypoxic neonatal mouse model, a significant enlargement of the right ventricle due to a combination of hypertrophy and proliferation of cardiomyocytes accompanied by a decrease in ceramide levels, increase in the levels of dihydroceramide, and a decrease in the expression of DEGS1 gene<sup>114,115</sup>. Likewise, lung and colon cancer models of hypoxia have shown increased levels of dihydroceramides mediated by inhibition of DEGS1 activity<sup>116</sup>. Since the desaturation reaction requires oxygen as electron acceptor, it is not unexpected that hypoxia inhibits DEGS1 activity and ceramide accumulation. However, Kang *et al.* have demonstrated that acute hypoxia increases ceramide levels *via* the *de*



*de novo* pathway in SH-SY5Y neuroblastoma cells, which leads to ceramide-dependent apoptosis<sup>117</sup>. In all, these data underscore the role of the *de novo* pathway of ceramide synthesis and DEGS1 as key biosensors to hypoxia.

### **G. Aims of the study:**

p53 protein encoded by the human gene *TP53* is a key tumor suppressor mutated in over 50% of human cancers<sup>118</sup>. Hypoxic stress, resulting from inadequate supply of oxygen to the rapidly growing solid tumors, acts as a potent physiological inducer and selector for the p53 mutant clones, conferring an aggressive phenotype for solid tumors<sup>119–124</sup>.

Since previous studies from our lab showed that in p53-dependent systems ceramide is regulated by p53 and functions downstream of it and that in p53-independent systems, such as cytokine-mediated apoptosis, ceramide functions independently of p53, we decided to examine the corresponding roles of p53 and ceramide in hypoxia.

*Here, we hypothesize that hypoxia induces p53-dependent ceramide accumulation followed by apoptosis in HCT-116 colon cancer cells, whereas in the absence of p53, HCT-116 colon cancer cells resist hypoxia-induced apoptosis and that this may be circumvented by exogenously administered ceramide.*

We aim to understand the connection between p53 and ceramide in the apoptotic pathway that takes place in the response to hypoxia. We will first determine the biological response to hypoxia in both p53-proficient and p53-deficient HCT-116 colon carcinoma cells. We will then study the p53-dependent regulation of ceramide

metabolism in response to hypoxia by measuring ceramide accumulation, characterizing the different ceramide metabolites, and measuring the expression of key enzymes involved in ceramide biosynthesis and breakdown in both p53-proficient and p53-deficient cells. We will also evaluate the effect of enzymatic down-regulation on the biological response to hypoxia through the administration of adequate pharmacological inhibitors. Finally, we will study the impact of exogenous ceramide administration on the cellular response to oxygen deprivation, notably in HCT-116 p53<sup>-/-</sup> cells. Our findings will provide clues for the possibility to adopt the modulation of ceramide metabolism as a potential sphingotherapy targeting hypoxia-resistant p53-deficient clones.

## CHAPTER II

### MATERIALS AND METHODS

#### **A. Cell culture**

HCT-116 is a human colon cancer cell line (was purchased from the American Tissue Culture Collection) that harbors a mutation in codon 13 of the KRAS proto-oncogene driving its uncontrollable proliferation.

HCT-116 p53<sup>+/+</sup> cells, naturally express p53 protein (Dr. Carlos Maria Galmarini, PharmaMar, Madrid, Spain). The *p53* gene was inactivated in HCT-116 p53<sup>-/-</sup> cells by homologous recombination. HCT-116 p53<sup>-/-</sup> cells were cultured in Dulbecco's Modified Eagle's Medium-high glucose, with 10% Fetal Bovine Serum (FBS), 1% Penicillin/Streptomycin, 1% sodium pyruvate and 1% nonessential amino-acids. HCT-116 p53<sup>+/+</sup> were cultured in Roswell Park Memorial Institute (RPMI 1640), with 10% Fetal Bovine Serum (FBS), 1% Penicillin/Streptomycin, 1% sodium pyruvate. Cells were incubated at 37°C, 5% CO<sub>2</sub> and passaged twice a week.

#### **B. Cell viability measurement by MTT**

HCT-116 p53 proficient (p53<sup>+/+</sup>) and p53 deficient (p53<sup>-/-</sup>) colon cancer cells were seeded in 96 well plates at a density of 5000 cell/well in 100µL of FBS-supplemented medium and incubated in hypoxic (1% O<sub>2</sub>) or normoxic (21% O<sub>2</sub>) conditions. The effect of hypoxia on cell viability was evaluated with the MTT (3-(4,5-dimethylthiazol-

2-yl)-2,5-diphenyltetrazolium bromide) assay. The conversion of the yellow tetrazolium salt, MTT, to the purple formazan dye is dependent on mitochondrial activity. 30  $\mu$ L of a stock solution of MTT (5 mg/ml in PBS, Sigma) was added to 100  $\mu$ L of culture medium/well, and the mixture was incubated for 4 h at 37°C in a humidified atmosphere containing 5% CO<sub>2</sub>. The crystals of formazan were then dissolved with Dimethyl sulfoxide (DMSO, Sigma), and reduced MTT levels were determined by measuring absorbance at 595 nm.

### **C. Flow Cytometric Analysis of the DNA Content**

HCT-116 cells were seeded in 6 well plates at a density of 150,000 cells/ well, incubated in hypoxic or normoxic conditions, and then harvested along with their supernatant. Cells were subsequently permeabilized with 70% ethanol, treated with 1% RNase, and finally stained with propidium iodide solution.

Analysis of cells distribution in the sub G<sub>0</sub>, G<sub>1</sub>, S, and G<sub>2</sub>/M phases of the cell cycle was performed on a BD FACSAria SORP flow cytometer, operated by BD FACS DIVA software. Cells less intensely stained than G<sub>1</sub> cells (sub G<sub>0</sub> cells) in flow cytometric histograms are considered as apoptotic cells.

### **D. Measurement of ceramide levels by DGK assay**

In order to define the role of ceramide in the p53-mediated response to hypoxia, total cellular lipids were collected from HCT-116 cells p53<sup>+/+</sup> and p53<sup>-/-</sup> at each time point by the Bligh and Dyer method<sup>117</sup>.

Lipids were subsequently used for phosphate measurements or diacylglycerol kinase (DGK) assay. This assay depends on the phosphorylation of diacylglycerol and ceramide by the transfer of phosphate from adenosine triphosphate, labeled on the gamma phosphate group with  $^{32}\text{P}$  (ATP, [ $\gamma$ - $^{32}\text{P}$ ]). This reaction generates radioactive phosphatidic acid and ceramide phosphate, respectively. The radiolabeled products were visualized by thin layer chromatography, scraped from the plates, quantitated by scintillation counting, and normalized to internal phosphate levels.

### **E. Liquid chromatography mass spectrometry (LC/MS)**

HCT p53 (+/+ and -/-) cells were seeded in T25 flasks at a density of 500,000 cells/flask, and subsequently grown in hypoxia or normoxia. At indicated time points, cells were scraped, harvested along with their supernatant, and washed with PBS. Lipids were extracted and sphingolipid levels were quantified by LC/MS using the API 4000 LC-MS/MS triple-stage quadrupole mass spectrometer operating in a multiple reaction monitoring positive ionization mode. Levels of sphingomyelin, sphingosine, S1P, ceramide species and C1P were normalized to protein cellular content and expressed in picomoles per nanogram of protein.

### **F. RNA extraction, reverse transcription, and quantitative Real-Time PCR**

#### ***1. RNA extraction***

For mRNA expression studies, total RNA was extracted from HCT-116 cells subjected to hypoxia or normoxia at the indicated time points (4, 6, 8, 24, 48 and 72 h) using the RNA isolation kit “RNeasy Mini Kit” (Qiagen), following manufacturer’s instructions.

## **2. Reverse transcription of RNA to cDNA**

The obtained RNA was reverse transcribed to cDNA using QuantiTech Reverse Transcription Kit (Qiagen) according to the manufacturer's protocol. First, potential genomic DNA (gDNA) was eliminated by treating the RNA sample with the gDNA Wipeout Buffer. The reverse-transcription reaction was carried-out using a master mix containing: Quantiscript reverse transcriptase, Quantiscript RT buffer, and RT primer mix. RNA was incubated with the prepared master mix at 42°C for 15 min, then at 95°C for 3 minutes to inactivate the reverse transcriptase.

## **3. Quantitative real-time PCR (qRT-PCR)**

For each transcript reaction, a master mix was prepared by combining 5 µL of iTaq Universal SYBR Green Supermix (Bio-Rad), 1µl of each forward and reverse primer (10uM), and 2µl nuclease free water. In each well of a 96-well PCR plate (Bio-Rad), 9 µl of the master mix were dispensed followed by 1µl of cDNA. Each sample was loaded in duplicates. PCR plate was sealed with an adhesive sealer, centrifuged for one minute and loaded into a BioRad CFX 96 thermocycler, using appropriate thermal cycling protocols. The obtained data were analyzed using the  $2^{-\Delta C_t}$  calculation method. The  $\beta$ -actin gene was used as internal reference control to normalize relative levels of gene expression. mRNA expression levels of *DEGS1* and *SphK1*, two key enzymes involved in ceramide anabolism and catabolism respectively, were evaluated following incubation in hypoxic or normoxic conditions. To this end, the following primers were ordered from Macrogen.

**Table 1. Primer sequences of *β-actin*, *DEGS1* and *SphK1***

Gene	Forward Primer	Reverse Primer
<i>β-actin</i>	CTGGCACCACACETTCTA	AGCACAGCCTGGATAGCAAC
<i>SphK1</i>	CGCCGCAGGGAATGACACC	GCCTGTCCCCCAAAGCATAAC
<i>DEGS1</i>	CCAACATTCTGGAAAAAGTCTTC	GCCTCTTCATTCTTGAGTAGGGA

### **G. Protein extraction and western blot analysis**

HCT-116 cells differentially expressing p53 were seeded in T25 flasks (500,000 cells/flask), then incubated in hypoxic conditions for 24, 48 and 72 hours. Cells were scraped and pelleted along with their supernatant at indicated time points.

Proteins were extracted using Laemmli buffer and their concentration was determined with the Bio-Rad dye-binding assay as per company instructions, using bovine serum albumin as standards. 30µg of proteins were resolved on polyacrylamide gel, and gel migration was carried-out at 100mV for 90 minutes in a 1X migration buffer. The Prism Ultra Protein Ladder was used as a molecular weight standard. After migration, proteins were electro-transferred onto PVDF (poly vinylene difluoride) membranes (Bio-Rad) in 1X transfer buffer using a Bio-Rad trans-blot cell.

PVDF membranes were then blocked in 5% milk prepared in 1X TBS-Tween for two hours. Immunoblotting was performed at 4°C overnight using appropriate primary antibodies. The next day, membranes were washed with 1X TBST, and subsequently incubated with appropriate HRP (horse reddish peroxidase) secondary antibodies for 1 hour at room temperature. Serial washing steps in 1X TBST were again performed. Protein bands were visualized through the BIORAD chemiDocMP imaging System

using Clarity™ ECL Western Blotting Substrate (Bio-Rad). Bands were quantified using ImageJ software, and protein expression was normalized to that of  $\beta$ -tubulin.

**Table 2: List of primary antibodies**

Product Code	Description
SAB4200715	Anti- $\beta$ -tubulin antibody
ab8245	Anti-GAPDH antibody
SAB2100559	Anti-DEGS1 antibody
ab191217	Anti-PARP antibody

#### **H. Statistical analyses**

MTT and cell cycle were performed in three independent experiments. Western blot, RTPCR and LC/MS experiments were repeated twice. Data are mean of independent experiments  $\pm$  S.D. Statistical analyses were performed by means of GraphPad Prism 8 software (GraphPad Software, San Diego, CA). p values were calculated using the unpaired Student's t-test. Differences were considered statistically significant when  $p < 0.05$  (\*,  $p < 0.05$ ; \*\*,  $p < 0.01$ ; \*\*\*,  $p < 0.001$ ).



## CHAPTER III

### RESULTS

#### **A. Defining the role of p53 in the cellular response to hypoxia**

In order to determine the role of p53 in the cellular response to hypoxia, HCT-116 p53 proficient (p53<sup>+/+</sup>) and deficient (p53<sup>-/-</sup>) cells were incubated in hypoxic conditions. We first validated the HCT-116 cellular models for p53 expression level, and then studied the hypoxia-induced response in HCT-116 cells differentially expressing p53.

##### ***1. Validation of HCT-116 cellular models***

HCT-116 p53<sup>+/+</sup> cells, typically express p53 protein. HCT-116 p53<sup>-/-</sup> cells derive from HCT-116 cells where the two p53 alleles have been sequentially disrupted by homologous recombination, which consists of inserting two promoter-less targeting vectors, each containing a geneticin- or hygromycin-resistance gene in place of the genomic p53 sequences. The models were validated for p53 expression level by western blot. Results showed that only HCT-116 p53<sup>+/+</sup> cells express p53, unlike HCT-116 p53<sup>-/-</sup> cells that showed no p53 protein expression (Fig. 10).

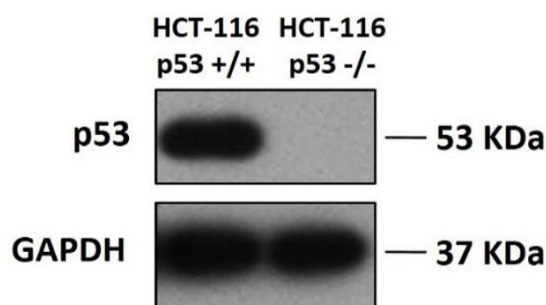


**Figure 10.** The expression level of p53 in HCT-116 p53<sup>+/+</sup> and p53<sup>-/-</sup> cells. Western blot analysis was performed in order to assess p53 protein expression under physiological conditions in HCT-116 p53<sup>+/+</sup> and p53<sup>-/-</sup> cells. GAPDH was used as an internal reference control.

## **2. Hypoxia-induced response in HCT-116 p53<sup>+/+</sup> and p53<sup>-/-</sup> cells**

Hypoxia-induced response in HCT-116 cells was first evaluated using MTT assay that was performed on HCT-116 cells differentially expressing p53 in order to assess their viability upon 24, 48 and 72 hours of incubation in hypoxic conditions.

This assay showed a substantial reduction in the viability of HCT-116 p53<sup>+/+</sup> cells upon exposure to hypoxia, starting at 48 hours and becoming significant at 72 hours. In contrast, The viability of HCT-116 p53<sup>-/-</sup> cells was not affected by the hypoxic stress (Fig.11.A). Thus, this strongly implies that p53 plays an important role in mediating hypoxia-induced decrease in cellular viability.

To further elucidate the mechanism responsible for the decrease in the cellular viability observed in p53 proficient cells, cells were permeabilized, DNA was stained with propidium iodide, and the percentage of cells in each phase of the cell cycle was assessed based on the cellular DNA content, using BD FACSAria SORP flow cytometer.

Changes in the cells distribution were only observed in the SubG0 population. SubG0 is the phase in which DNA is fragmented, reflecting programmed cell death, alternatively named apoptosis. Unlike p53<sup>-/-</sup> cells, p53-proficient (p53<sup>+/+</sup>) cells showed a significant increase in DNA fragmentation (% cells in SubG0 phase) upon 72 hours of hypoxic exposure accompanied by PARP cleavage, indicating an apoptotic response (Fig.11.B and C).

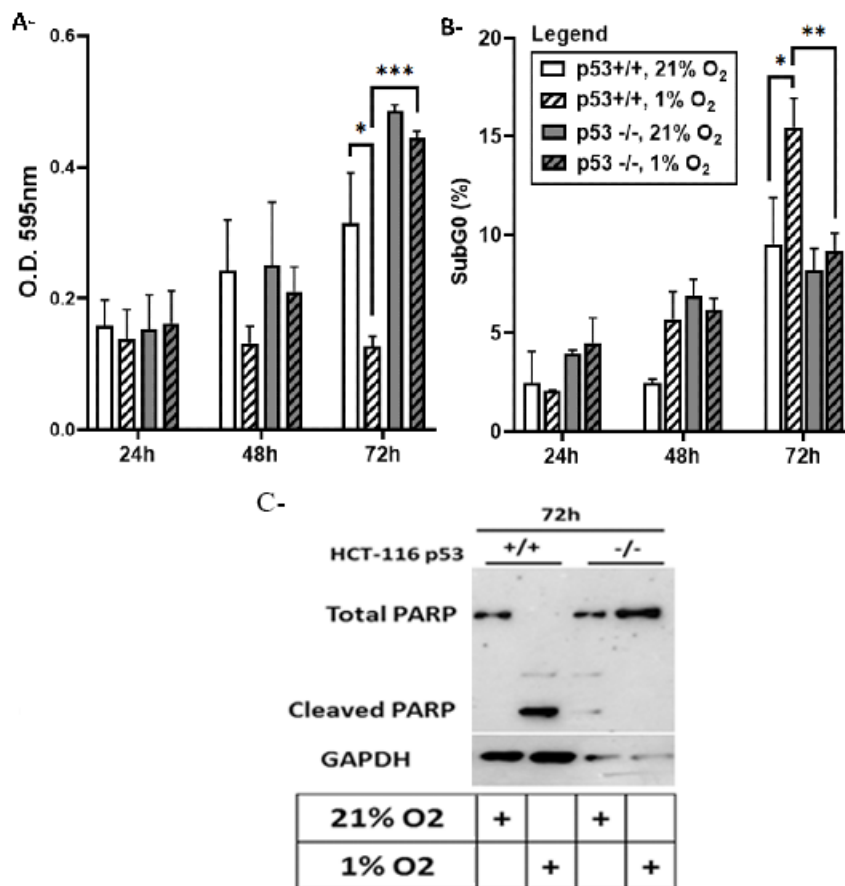


**Figure 11. Response of HCT-116 cells to hypoxia.** A- MTT assay was performed on HCT-116 p53<sup>+/+</sup> (white) and <sup>-/-</sup> (grey) cells after 24, 48 and 72 hours of incubation in normoxia (21% O<sub>2</sub>, plain) or hypoxia (1% O<sub>2</sub>, patterned). The optical density (O.D.) was measured at 595 nm. Values represent the average of three independent experiments ± S.D. B- % cells in subG0 phase of the cell cycle as measured by flow cytometry. Each column represents the mean ± S.D. of three independent experiments. \* p < 0.05, \*\*p < 0.01, \*\*\*p < 0.001. C- Analysis of PARP cleavage by western blot. Data are representative of 2 independent experiments.

Therefore, we were able to conclude that in the absence of p53, HCT-116 cells were able to resist the hypoxia-induced apoptosis. Hence, p53 is required for the apoptotic response to hypoxic stress.

## **B. Defining the ceramide response to hypoxia in the presence and absence of p53**

The previous result highlighted the role of p53 in mediating the apoptotic response to hypoxic stress. Ceramide, a signaling sphingolipid, has been previously described as a collaborator with p53 in the stress response<sup>67</sup>.

As discussed above ceramide acts mostly downstream of p53 protein through post-transcriptional regulation or through several potential mediators. It can, on the other hand, induce apoptosis independently of p53. It is, therefore, crucial to elucidate the role of ceramide in the hypoxic response in our present model.

### ***1. Changes in total ceramide levels in response to hypoxia measured by DGK assay***

The DGK assay was performed in order to measure total ceramide content upon exposure to hypoxia for 24, 48 and 72 hours. Radioactive phosphorylated ceramide levels were quantified using a liquid scintillation counter and normalized to total lipid phosphates.

In response to cellular stressors, including hypoxia, ceramide is expected to be induced and mediate growth suppressive responses. Surprisingly, in our cellular model, HCT-116 p53<sup>-/-</sup> cells, which were shown to be resistant to hypoxia-induced apoptosis, demonstrated a significant ceramide accumulation at 72 hours of exposure to 1% O<sub>2</sub>

compared to their normoxic time-matched control. However, in the presence of p53, hypoxia-induced apoptotic cell death occurred after prolonged incubation (72h) in 1% O<sub>2</sub>; yet, this was not accompanied nor preceded by any significant ceramide accumulation (Fig.12).

Since p53<sup>+/+</sup> cells that undergo apoptosis were not associated with ceramide accumulation, yet in the absence of p53, ceramide accumulates with sustained survival, therefore we postulated that ceramide might be dissociated from the p53-dependent biological response to hypoxia and that in the absence of p53, a fraction of ceramide might be catabolized into a pro-survival sphingolipid reverting ceramide induced effects.

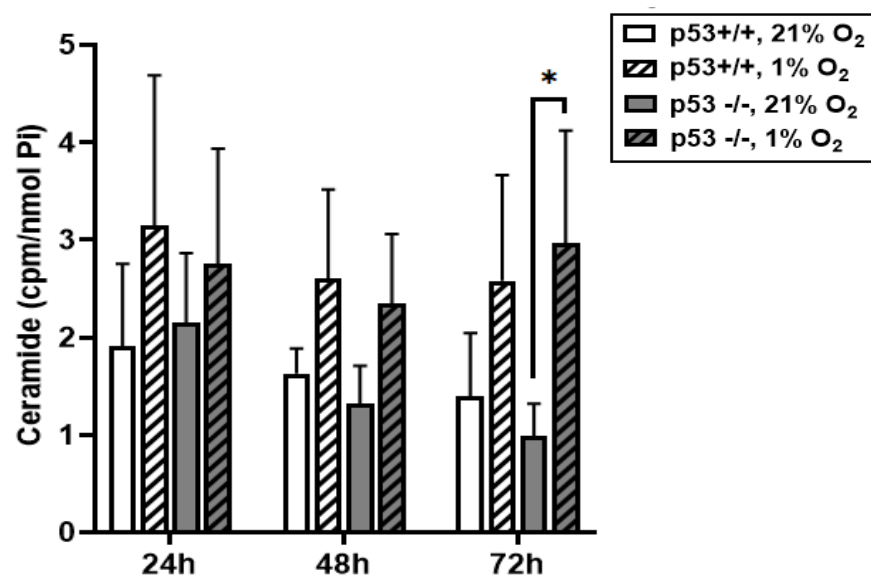


**Figure 12. Ceramide accumulation upon hypoxia in HCT-116 p53<sup>+/+</sup> and p53<sup>-/-</sup> cells.** HCT-116 cells were exposed to normoxia (21% O<sub>2</sub>) or hypoxia (1% O<sub>2</sub>) for 24, 48 and 72 hours. Ceramide levels were quantified at indicated time points by DGK assay and normalized to phosphate content. Values are the average of three independent experiments with standard deviations. \* p < 0.05 is a significant difference with respect to normoxia.

## ***2. Examine the association between ceramide metabolic pathways and the biological response to hypoxia***

In this section, we aimed to understand whether ceramide is responsible for the resistance to hypoxia observed in the absence of p53 and describe the role of ceramide metabolic pathways in this response. Hence, we selected four different enzymes responsible for ceramide biosynthesis or catabolism, and evaluated the effect of their inhibition on the biological response to hypoxia. GW4869 is a selective inhibitor of neutral sphingomyelinase that is involved in the sphingomyelin hydrolysis pathway. Desipramine is a specific inhibitor of A-SMase, which contributes in part to the salvage pathway of ceramide biosynthesis. FB1 is a specific inhibitor of ceramide synthases, which are enzymes involved in the *de novo* and salvage pathways of ceramide generation. SK1-I is a selective inhibitor of sphingosine kinase 1 responsible for the phosphorylation of sphingosine, a catabolite of ceramide, into sphingosine 1-phosphate, a signaling sphingolipid with a pro-tumor signature.

### **a. Targeting neutral sphingomyelinase (NSMase) using GW4869, and examining its impact on the cellular response of HCT-116 cells to hypoxia**

In an attempt to understand whether the resistance to hypoxic stress observed in p53-deficient cells implied the engagement of the sphingomyelin hydrolysis pathway, HCT-116 cells differentially expressing p53 were treated with 1.5 mM of GW4869 prior to their incubation in a hypoxic chamber for 24, 48 and 72 hours.

The effect of NSMase inhibition on the cellular response to hypoxia was evaluated by studying cell viability and apoptosis, through MTT assay and flow cytometric analysis

of the SubG0 population, respectively. The values obtained from the GW4869-treated cells were normalized to those of the vehicle-treated control cells and data were presented as mean of ratios (treated/control) from three independent experiments  $\pm$  S.D. We found no changes in cell viability (Fig.13.A) nor in apoptotic response (Fig.13.B) in both HCT-116 models subjected to hypoxia, upon treatment with GW4869 (fold change treated/control  $\approx$  1).

These results indicate that either the ceramide accumulation observed in the absence of p53 is not due to NSMase activation or, if it is, then it is dissociated from the resistant response to hypoxia.

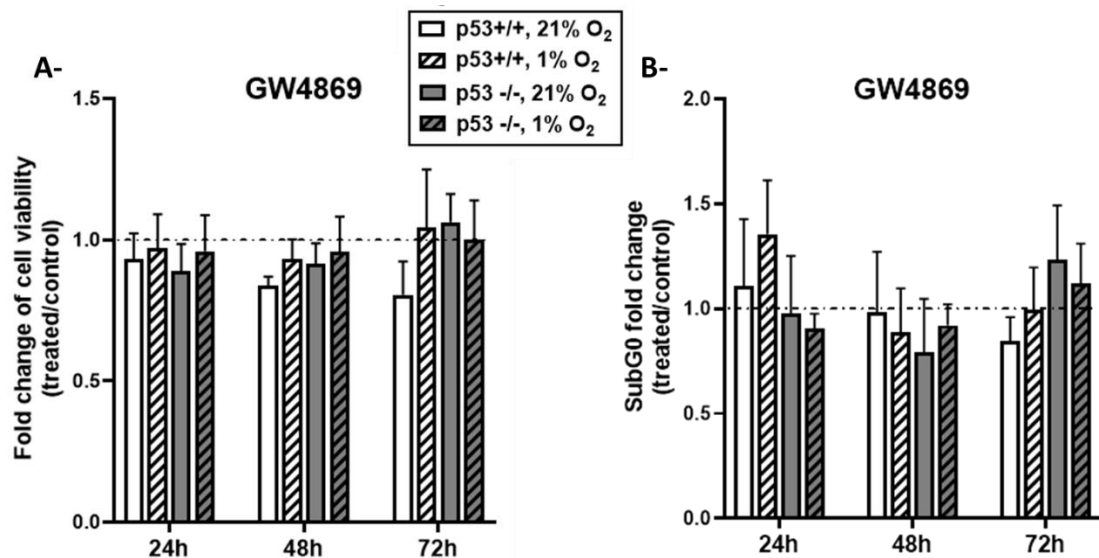


**Figure 13. Evaluation of the effect of GW4869 on the response of HCT-116 cells to hypoxia.** A- Fold change of the cell viability in the GW4869-treated cells/control. MTT assay was performed and optical density (O.D.) was measured at 595 nm, values represent the ratios of O.D. obtained from the GW4869-treated cells over their vehicle-treated control. B- Fold change of the % of apoptotic cells in the GW4869-treated cells/control. The percentage of cells in the subG0 phase of the cell cycle was quantified by flow cytometry, values represent the ratios of the percentages obtained from GW4869-treated cells over their vehicle-treated control. Each column represents the mean  $\pm$  S.D. of the ratios calculated from three independent experiments.

b. Targeting acid sphingomyelinase (ASMase) using desipramine and examining its impact on the cellular response of HCT-116 cells to hypoxia

In order to assess whether ASMase pathway of ceramide synthesis contributes to the biological response to hypoxia, HCT-116 cells were pretreated with desipramine (10  $\mu$ M), then exposed to hypoxia/normoxia. MTT assay and FACS analyses of the DNA content were performed at indicated time points. As observed with GW4869, we did not observe any changes in the cellular viability (Fig.14.A) nor in the apoptotic profile (Fig.14.B) upon desipramine treatment in both cellular models incubated in hypoxia and normoxia (fold change treated/control  $\approx$  1). This implies that ASMase activity is not required for the ceramide-mediated effects in the absence of p53, or that the ceramide generated through this pathway is completely dissociated from the p53-independent response to hypoxia.



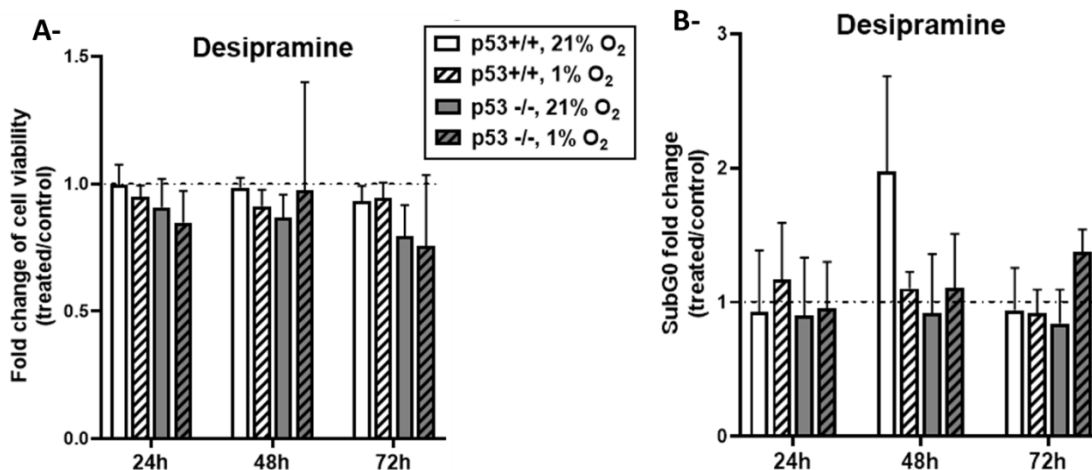


**Figure 14. Evaluation of the effect of desipramine on the response of HCT-116 cells to hypoxia.** A- Fold change of the cell viability in the desipramine-treated cells/control. MTT assay was performed and optical density (O.D.) was measured at 595 nm, values represent the ratios of O.D. obtained from the desipramine-treated cells over their vehicle-treated control B- Fold change of the % of apoptotic cells in the desipramine-treated cells/control. The percentage of cells in the subG0 phase of the cell cycle was quantified by flow cytometry, values represent the ratios of the percentages obtained from desipramine-treated cells over their vehicle-treated control. Each column represents the mean  $\pm$  S.D. of the ratios calculated from three independent experiments.

c. Targeting ceramide synthases and sphingosine kinase 1 and examining the impact of their inhibition on the response of HCT-116 cells to hypoxia.

In order to determine if CerSs-mediated ceramide generation is responsible for the resistance observed in p53-deficient cells upon 72 hours of hypoxia, HCT-116 cells were treated with CerSs inhibitor, FB1 at 10  $\mu$ M, placed in 1% O<sub>2</sub>, and their response to the decrease in oxygen levels evaluated through MTT assay and flow cytometric analysis of DNA fragmentation. Results were plotted as fold change of treated samples over their vehicle-treated control. HCT-116 p53-deficient cells demonstrated a slight,

yet not statistically significant, decrease in cell viability of about 30 (Fig.15.A), and a preliminary increase in the percentage of apoptotic cells of about 25% upon 72 hours of exposure to hypoxia, compared to their p53<sup>+/+</sup> counterparts (Fig.15.B), in contrast to a relatively sustained cell viability in their p53-proficient counterparts. This signals a presumable role of CerSs-mediated ceramide generation in the p53-independent response to hypoxia.

Since the observed ceramide accumulation in p53-deficient cells was associated with improved survival of these cells, counter to the established role of ceramide in most cancers as a pro-apoptotic molecule, we decided to examine whether ceramide was being metabolized to one of its anti-apoptotic downstream products, S1P, generated by the successive actions of ceramidase and then SK1. First, we made use of the SK1 selective inhibitor, SK1-I, which, by itself, did not influence the viability (Fig.15.A) nor the apoptotic response (Fig.15.B) of either of the cell lines upon being subjected to a low oxygen tension. Since inhibiting SK1 was not able to revert the resistant phenotype, this suggested that an alternative pathway may be playing a role.

When treated with both inhibitors (FB1 and SK1-I), and in the absence of p53, HCT-116 cells were no longer able to tolerate the hypoxic stress and had a significant decrease in their cell viability probably by undergoing apoptosis. The decrease in cell viability reached 34%, 52% and 60% in p53-deficient cells as against 17%, 22% and 16% in the presence of p53 at 24, 48 and 72 hours respectively (Fig.15.A).

Correspondingly, the percentage of apoptotic population increased by around 4.3 folds and 3.1 folds in the p53<sup>-/-</sup> cells as compared to p53<sup>+/+</sup> cells, upon exposure to hypoxia for 48 and 72 hours, respectively (Fig.15.B).

Our results indicate that ceramide that accumulates in response to hypoxia in the absence of p53 and correlates with the resistance of these cells to hypoxia-induced cell death, is mostly synthesized by CerSs. When targeting CerSs for inhibition using FB1, two major pathways of ceramide synthesis are being affected:

- The *de novo* synthesis pathway
- The reacylation step of the salvage pathway.

A prolonged inhibition of CerSs will result in a cascade of changes in sphingolipid metabolism. Complex sphingolipids are driven to the salvage pathway in order to recycle ceramide. They are broken down into ceramide, subsequently deacylated into sphingosine which quits the lysosome; not able to be reacylated by CerSs due to its inhibition by FB1, sphingosine will be phosphorylated into the pro-survival lysophospholipid S1P. Inhibition of sphingosine phosphorylation through SK1-I shifts the sphingosine/S1P balance toward a critical accumulation of sphingosine, which is established as a proapoptotic sphingolipid.

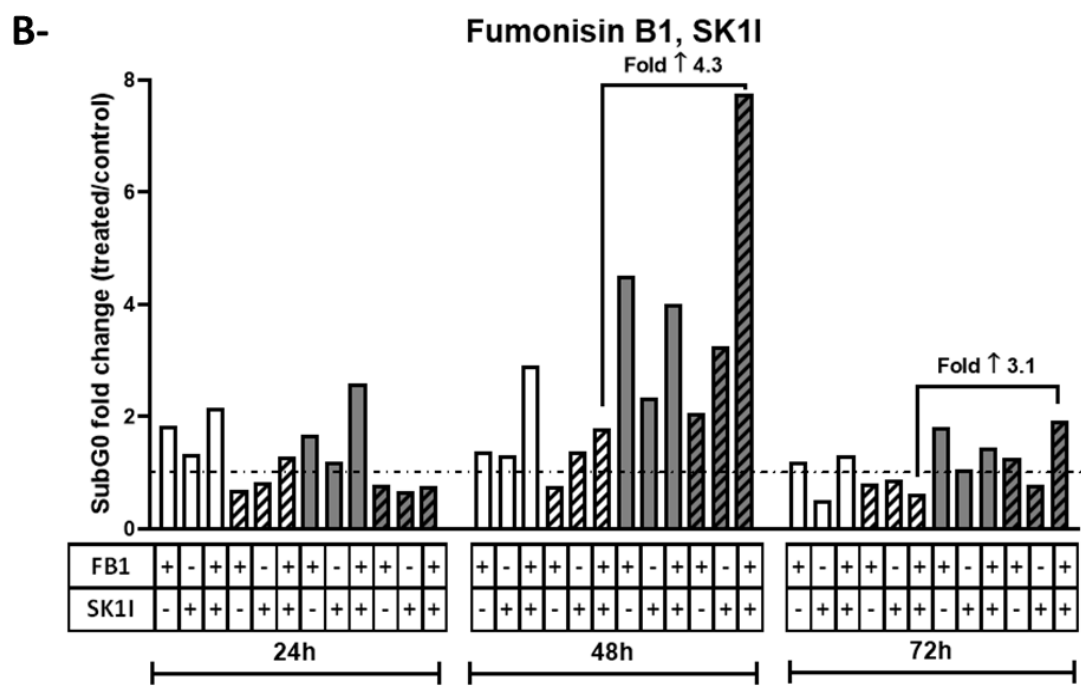
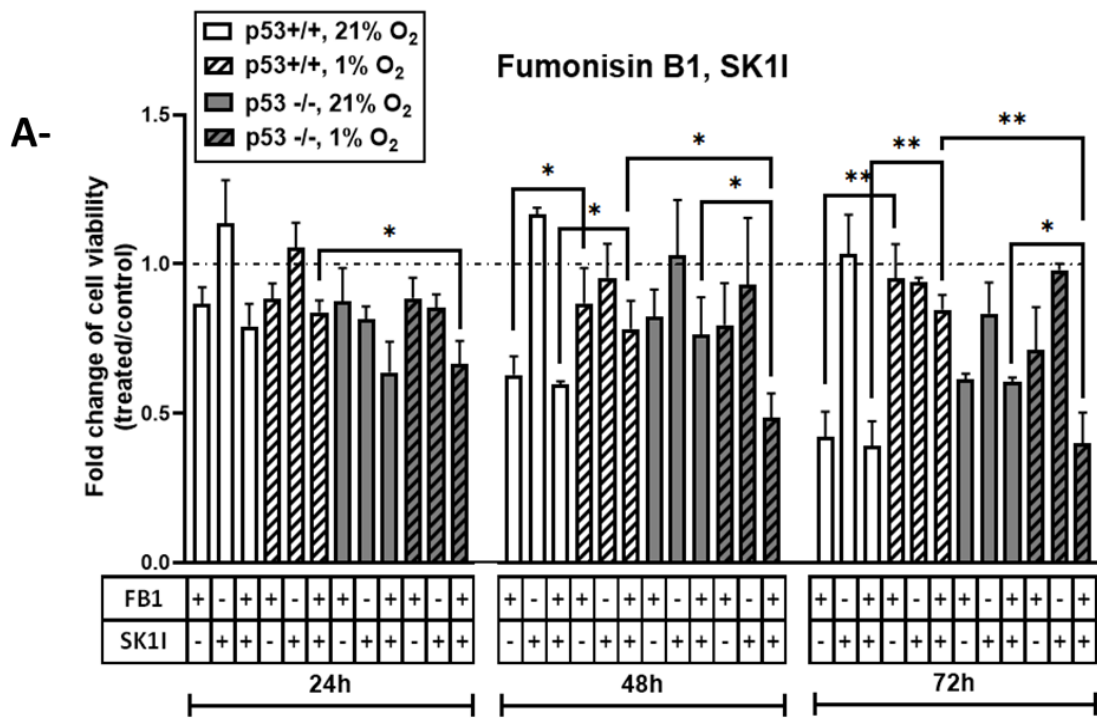


**Figure 15. Evaluation of the effect of fumonisin B1 or/and SK1-I on the response of HCT-116 cells to hypoxia.** A- Fold change of cell viability of the FB1/SK1-I-treated cells/control. MTT assay was performed and optical density (O.D.) was measured at 595 nm. The ratios of O.D. obtained from the FB1/SK1-I-treated cells over their vehicle-treated control were calculated. Each column represents the mean  $\pm$  S.D. of the ratios calculated from three independent experiments. B- Fold change (FB1/SK1-I-treated/control) of the % of apoptotic cells. The percentage of the subG0 population was quantified by flow cytometry. Each column is the ratio of the percentages obtained from FB1/SK1-I-treated cells over their control. Values represent a single experiment.

In our earlier findings (Fig. 11, 12) we reported that in the absence of p53, HCT-116 cells resisted hypoxia-induced apoptosis in correlation with ceramide accumulation. We then demonstrated that CerSs are potentially responsible for ceramide generation, and that a fraction of the accumulated ceramide is likely converted into the anti-apoptotic lipid S1P.

However, before concluding which ceramide metabolite drives the biological effects observed in our model, several points should be addressed:

- First, the DGK assay is not selective for ceramide. The DGK enzyme phosphorylates different substrates including diacylglycerol, ceramide and dihydroceramide. The phosphorylated products of the latter two metabolites cannot be separated by thin layer chromatography. Hence, the observed “ceramide accumulation” may account for the generation of ceramide and/or dihydroceramide.
- Second, as mentioned above, since the acylation reaction catalyzed by CerSs covers two compartmentally separated pathways for ceramide synthesis, CerS inhibition using FB1 may affect either the *de novo* synthesis or the salvage

pathway, or both of them. It may also influence several ceramide metabolites including dihydroceramide, sphingosine and complex sphingolipids. Hence, further verification is required to determine which metabolite(s) is (are) likely to be involved in the ceramide-mediated response to hypoxia.

- Finally, previous studies carried out on multiple primary and transformed cell types, and on a hypoxic animal model of cyanosis, have demonstrated that DEGS, the enzyme that desaturates dihydroceramide into ceramide in the last step of the *de novo* synthesis pathway, fulfills the criteria of an oxygen sensor<sup>114,116,126</sup>.

In light of the above, and in order to elucidate the role of the *de novo* synthesis pathway of ceramide generation in the biological response to hypoxia, we assessed the genetic and protein expression of the dihydroceramide desaturase enzyme (DEGS1) in HCT-116 cells under low oxygen tension, through qRT-PCR and western blot, respectively. We subsequently screened for the different ceramide species through LC/MS.

Briefly, cells were incubated in normoxic or hypoxic conditions, and harvested at the indicated time points. RNA was extracted and reverse transcribed, and quantitative real-time PCR was carried out on the obtained cDNA. Cycle threshold (CT) was determined using CFX Manager 2.0 software (Bio-Rad).  $2^{-(CT_{DEGS1} - CT_{\beta-actin})}$  was calculated, and data were presented as  $\log(2^{-\Delta CT(\text{hypoxia})} / 2^{-\Delta CT(\text{normoxia})})$ .

HCT-116 p53<sup>+/+</sup> cells demonstrated a trend to decrease DEGS1 mRNA expression, especially after 72 hours of incubation in hypoxic conditions. In contrast, in the absence of p53, DEGS1 mRNA expression was relatively maintained (Fig.16.A).

Likewise, DEGS1 protein expression was decreased in p53-proficient cells after 72 hours of being subjected to 1% O<sub>2</sub> but was however sustained in their p53-deficient counterparts (Fig.16.B and C).

Our present findings underscore the role of the desaturation step in the *de novo* synthesis pathway of ceramide generation in oxygen sensing and indicate a role for p53 in DEGS1 regulation.

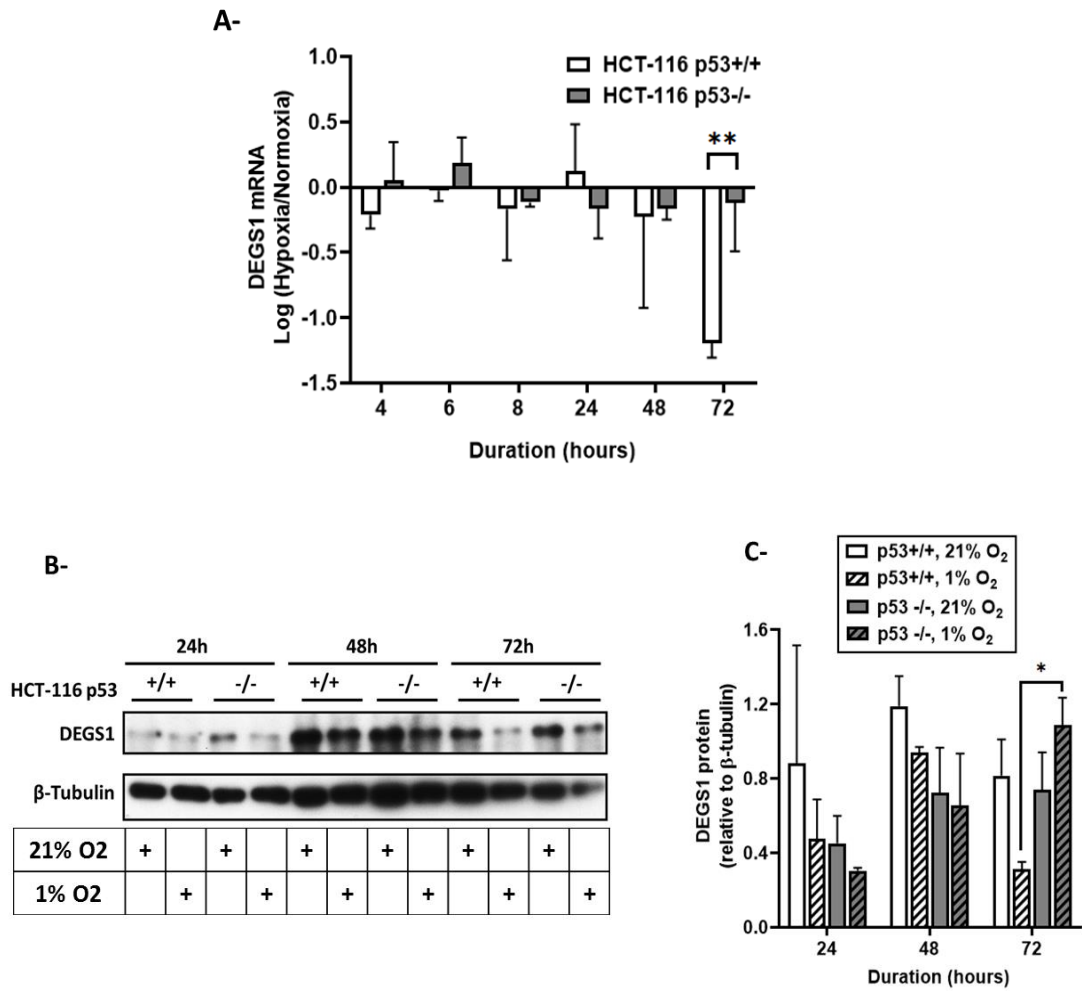


**Figure 16. Modulation of DEGS1 expression in response to hypoxia in both p53<sup>+/+</sup> and p53<sup>-/-</sup> HCT-116 cells.** A- Log Fold change (hypoxia/normoxia) of DEGS1 mRNA expression assessed by qRT-PCR. Values represent the average of two independent experiments  $\pm$  S.D. B- Analysis of DEGS1 protein expression by western blot. C- Normalization of DEGS1 protein expression to that of  $\beta$ -tubulin. Each column represents the average of two independent experiments  $\pm$  S.D.



### 3. Changes in the levels of ceramide species upon hypoxia

DEGS1 expression data support a role for it in the hypoxia-induced p53-independent ceramide accumulation observed through DGK assay. In order to further elucidate which ceramide species were accumulating in response to hypoxia, we analyzed the sphingolipid profile of HCT-116 cells using LC/MS.

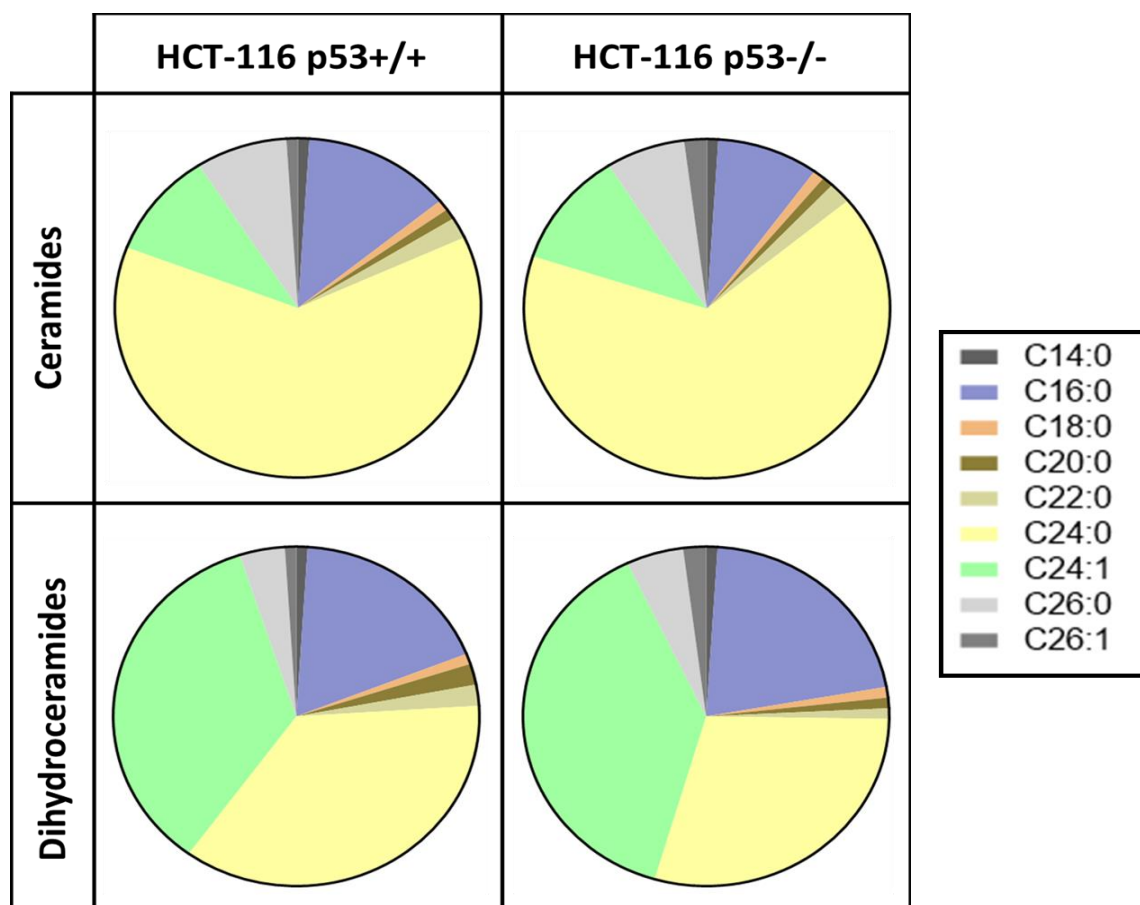


**Figure 17. Ceramide and dihydroceramide species distribution in HCT-116 cells under physiological conditions.** Data represent the average calculated from two independent experiments of ceramide and dihydroceramide levels normalized to protein content (pmol/mg protein). No significant difference was detected between the p53-proficient and the p53-deficient cellular models.

Under physiological conditions, ceramide and dihydroceramide species were equally distributed in p53 deficient and p53 proficient HCT-116 cells with C24 being the most abundant between ceramide and dihydroceramide species (Fig.17). However, after incubation in hypoxia, ceramide levels significantly increased in the absence of p53 (Fig.18 and 19), which was concordant with the previous data of ceramide accumulation and DEGS1 expression.

According to their N-acyl chain lengths, ceramides are classified into medium (C12–14), long (C16–C18), very long (C20–C24), and ultralong (C26 and above) chain species<sup>127</sup>.

C14:0 and C16:0-Cer, synthesized by ceramide synthases 5 and 6, did not demonstrate any prominent changes in their levels upon exposure to hypoxia in either of the cellular models (Fig.18).

C18:0, C20:0 and C20:1-Cer, synthesized by ceramide synthases 1, 2 and 4, showed a significant accumulation in p53-deficient, but not in p53-proficient HCT-116 cells, upon 72 hours of exposure to hypoxia (Fig.18).

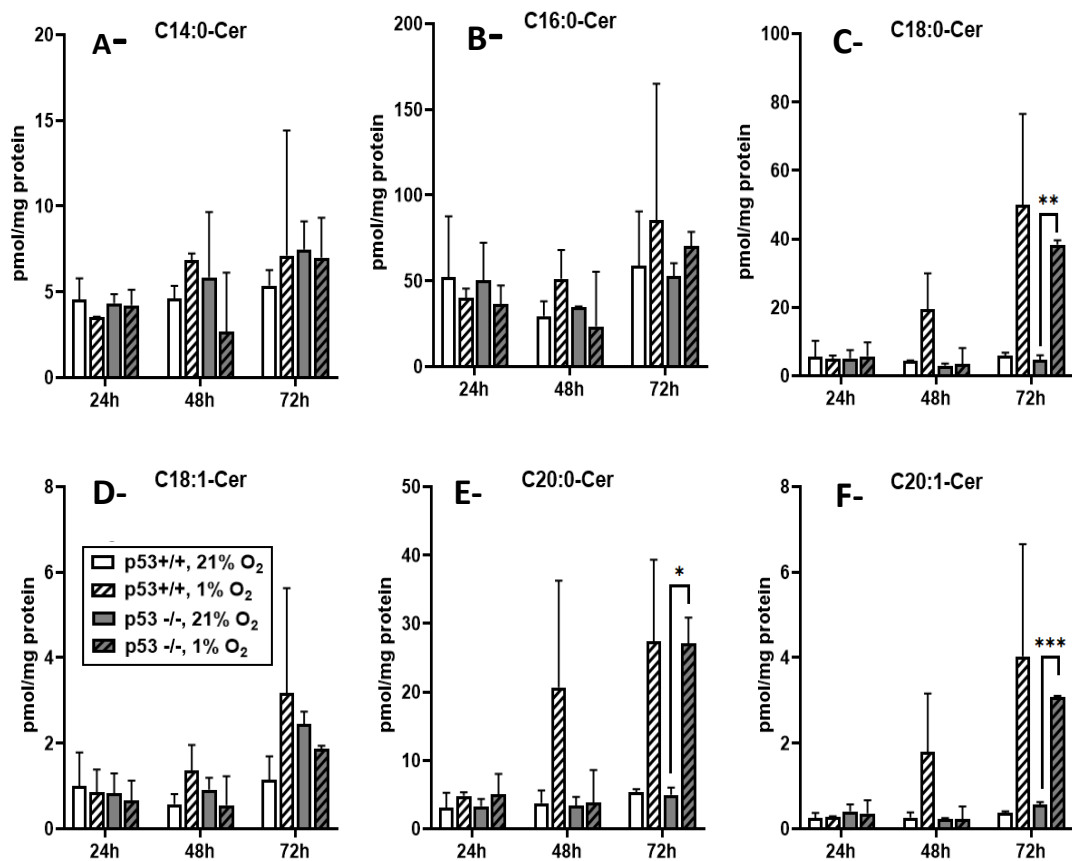


**Figure 18. Changes in the levels of medium and long chain ceramide species in HCT-116 cells subjected to hypoxia.** Different molecular species of ceramide were quantified by liquid chromatography-mass spectrometry and normalized to protein content (pmol ceramide/mg protein). Data is the average of two independent experiments  $\pm$  S.D. \* $p < 0.05$ ; \*\* $p < 0.01$ ; \*\*\* $p < 0.001$ .

Very long and ultralong ceramide species (C22:0, C22:1, C24:0, C26:0 and C26:1-Cer), synthesized by ceramide synthases 2 and 3 significantly accumulated under 1% O<sub>2</sub> in the absence of p53 (Fig.19).

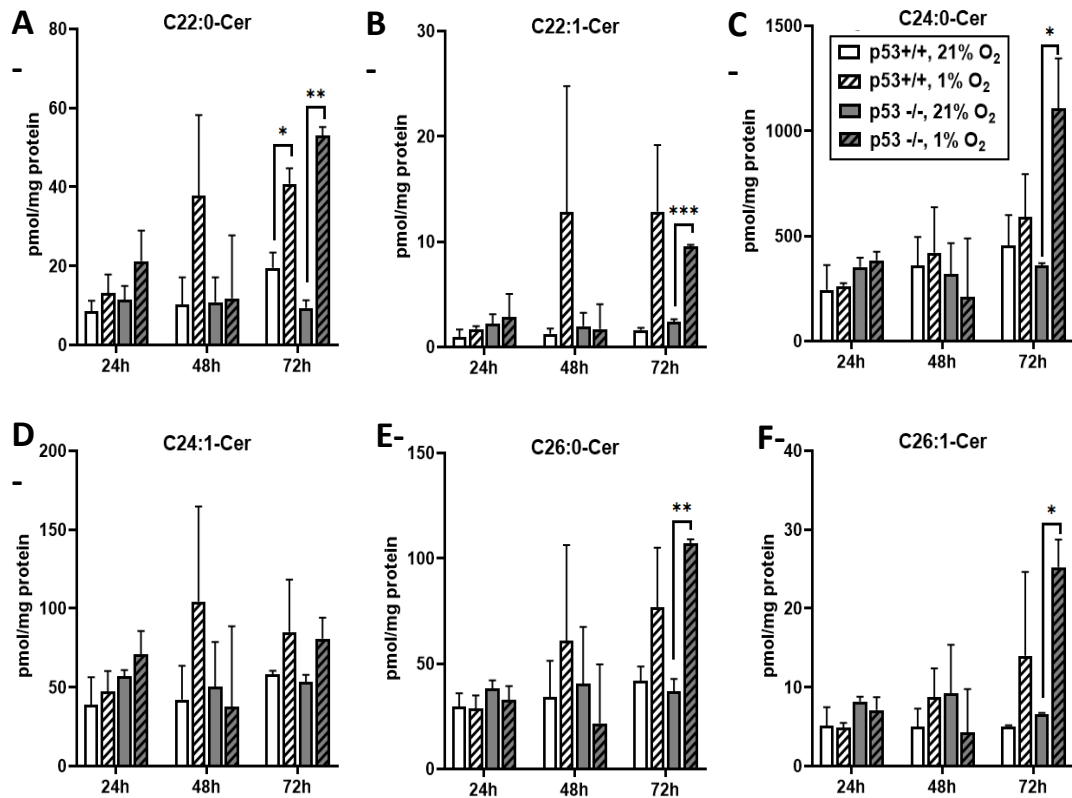


**Figure 19. Changes in the levels of very long and ultralong chain ceramide species upon hypoxia.** Different molecular species of ceramide were quantified by liquid chromatography-mass spectrometry and normalized to protein content (pmol ceramide/mg protein). Data is the average of two independent experiments  $\pm$  S.D. \* $p < 0.05$ ; \*\* $p < 0.01$ ; \*\*\* $p < 0.001$ .

#### *4. Changes in ceramide catabolism upon hypoxia*

One hypothesis that could explain the correlation of increased ceramide levels with resistance to apoptosis is its conversion to one of its anti-apoptotic metabolites. Thus, ceramide generated in p53<sup>-/-</sup> cells exposed to hypoxic conditions can be deacylated by ceramidases producing sphingosine and a fatty acid. The sphingosine can be phosphorylated giving rise to the pro-survival lipid, S1P, which may potentially contribute to the resistance of p53-deficient cells to hypoxia-induced apoptosis.

In order to further elucidate this mechanism, we measured the levels of sphingosine and S1P by LC/MS and the genetic expression of SK1. The notion of the dynamic balance between ceramide and S1P, termed as “sphingolipid rheostat”, has been a major focus in cancer therapy recently.

Unfortunately, S1P levels were not detected by LC/MS; however, interestingly, sphingosine levels were significantly decreased in p53-deficient cells, but not in p53-proficient cells, upon 72 hours of exposure to hypoxia compared to their normoxic time-matched control (Fig.20). This suggests, but does not confirm, that sphingosine might be further metabolized into S1P by SK1.

Correspondingly, SK1 mRNA expression was down-regulated in response to hypoxia in HCT-116 p53-proficient cells, and conversely upregulated in the absence of p53 with a significant difference observed at 72 hours (Fig. 20). Hence, we postulated that the ceramide generated in the absence of p53 was partially catabolized into the anti-apoptotic lipid, S1P, and contributed to the resistance of p53-deficient cells to hypoxia-induced apoptosis.

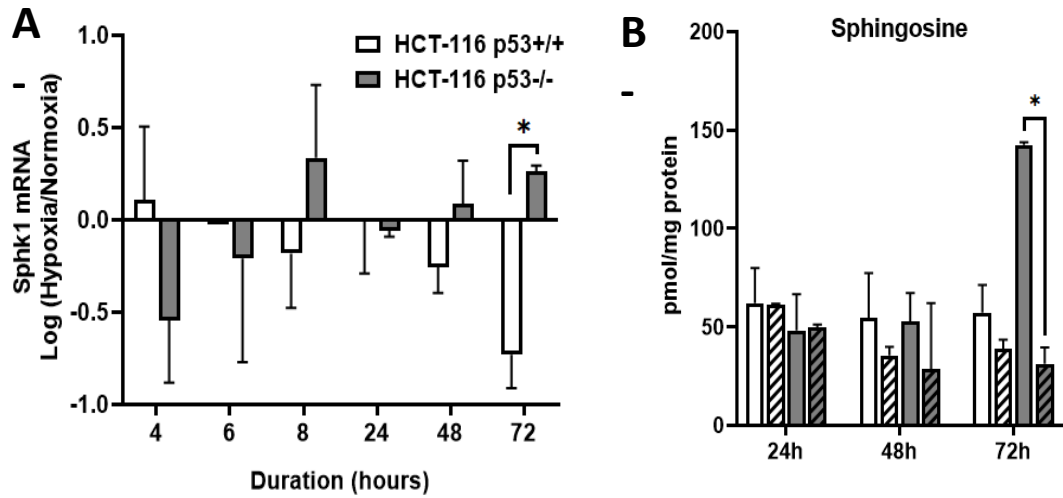


**Figure 20. Modulation of sphingosine kinase 1 (SK1) mRNA expression and sphingosine levels in response to hypoxia in both p53<sup>+/+</sup> and p53<sup>-/-</sup> HCT-116 cells.** A-Log Fold change (hypoxia/normoxia) of SphK1 mRNA expression assessed by qRT-PCR. Values represent the average of two independent experiments  $\pm$  S.D. B-Sphingosine was quantified by liquid chromatography-mass spectrometry and normalized to protein content (pmol sphingosine/mg protein). Data is the average of two independent experiments  $\pm$  S.D. \*p<0.05

### **C. Effect of exogenous C6 ceramide on the biological response to hypoxia of HCT-116 cells differentially expressing p53**

Our previous results suggested that the cellular fate of HCT-116 cells in response to hypoxia could be determined by the metabolic balance between two bioactive signaling sphingolipids, ceramide and S1P. The ceramide/S1P rheostat has been thoroughly discussed in the literature for its regulatory role in cancer pathogenesis and therapeutics<sup>128</sup>. Herein we propose that in response to hypoxia, and in the absence of p53, the proapoptotic lipid ceramide is being metabolized into a sphingolipid with opposing functions, S1P, which possibly drives the resistance of these cells to hypoxia. Hence, restoring the catabolized cellular ceramide alters the ceramide/S1P balance and potentially sensitizes the p53-deficient HCT-116 cells to hypoxia-induced cell death. This could be achieved through the administration of exogenous synthetic cell-permeable short chain ceramides (C2, C4, C6, and C8 ceramide) that get deacylated then re-acylated inside the cell through the addition of longer fatty acid chains to the sphingosine backbone, in order to generate endogenous longer chain ceramides<sup>129,130</sup>. Accordingly, HCT-116 cells differentially expressing p53 were treated with exogenous C6 ceramide and were then incubated in hypoxic conditions for 24, 48 and 72 hours. The subsequent cellular response was evaluated through cell viability assays (MTT) and the flow cytometric analysis of DNA fragmentation underlying the apoptotic response. Indeed, MTT results demonstrated that exogenous C6 ceramide was able to selectively decrease the viability of p53-deficient cells upon oxygen deprivation for 48 and 72 hours (Fig.21). This decrease in the cellular viability was accompanied with a significant increase in the percentage of apoptosis in p53-deficient cells upon 72 hours

of exposure to hypoxia compared to their p53-proficient counterparts and to their normoxic time-matched control, as revealed by the percentage of subG0 population analyzed on FACSARIA flow cytometer. This experiment indicated that tipping the balance in favor of ceramide changes the outcome from survival to apoptosis.

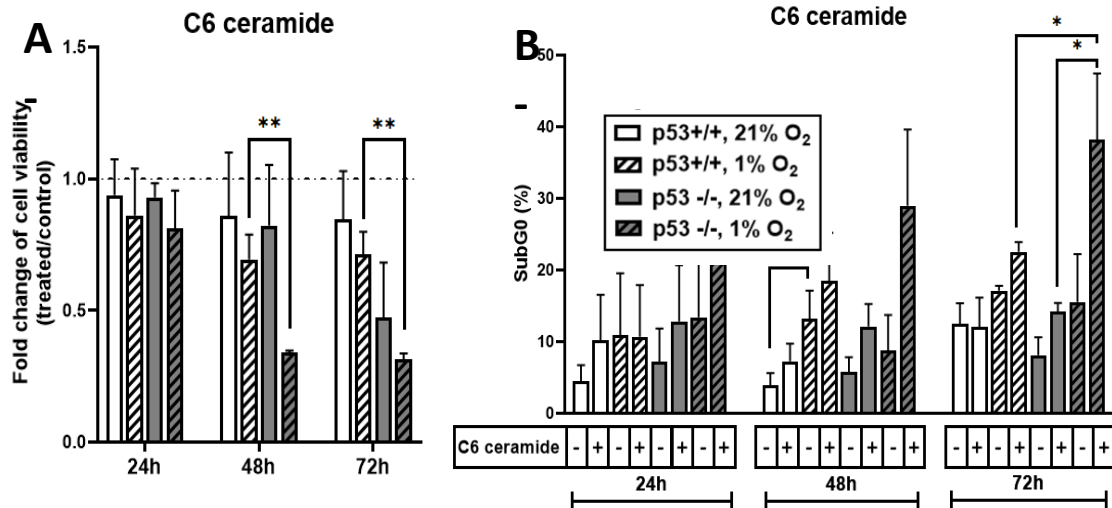


**Figure 21. Evaluation of C6 ceramide impact on the response of HCT-116 cells to hypoxia.** HCT-116 p53+/+ and -/- cells were pre-treated with exogenous C6 ceramide, MTT assay and flow cytometric analysis of the DNA content were performed after 24, 48 and 72 hours of incubation in normoxia (21% O<sub>2</sub>) or hypoxia (1% O<sub>2</sub>). A-Fold change of cell viability of the C6 ceramide-treated cells/control. MTT assay was performed and optical density (O.D.) was measured at 595 nm. The ratios of O.D. obtained from the C6 ceramide-treated cells over their vehicle-treated control were calculated. Each column represents the mean  $\pm$  S.D. of the ratios calculated from three independent experiments. B- % of apoptotic cells. The percentage of the subG0 population was quantified by flow cytometry. Each column represents the average  $\pm$  S.D. calculated from three independent experiments. \*p<0.05; \*\*p<0.01



## CHAPTER IV

### DISCUSSION

Hypoxia is a common feature of locally advanced solid tumors resulting from the vascular inability to meet the metabolic requirements of the exponentially proliferating cancer cells. As a result, high vascular heterogeneity arises, and gradients of oxygen concentration emerge. Knowing that p53 is a transcription factor involved in cell death, regions of severe hypoxia undergo programmed cell death in a p53-dependent manner. On the other side, in order to evade hypoxia-induced cell death, cancer cells undergo mutations in the *TP53* tumor-suppressor gene, losing the wild-type p53 proapoptotic function, and gaining the mutant p53 function, which is mainly involved in cancer progression. In colon cancer, *TP53* mutation is believed to occur at the time of transition from adenoma to cancer.

Hypoxic stress is one of the earliest driving forces that mutate *TP53* during tumorigenesis. It can additionally act as an environmental selector for the aggressive p53 mutants such that minor clones carrying nonfunctional alleles of the *TP53* gene overtake populations wild-type for *TP53* ultimately leading to tumor resistance.

Previous studies have shown that p53-deficient cells, even when cultured 1:1000 relative to p53 wild-type cells, can outgrow the p53 wild-type population in a hypoxic environment<sup>131</sup>.

Although several p53-targeted therapies aiming to restore WT p53 function upon p53 mutation have entered clinical trials, several limitations arose and hindered the efficacy of these approaches.

Since previous studies performed on irradiated MOLT-4 leukemia cells showed that ceramide acts downstream of p53 and mediates the apoptotic response to cellular stress, we hypothesized that ceramide might mediate the p53-dependent apoptotic response to hypoxia.

In order to test this hypothesis, we first studied the response of HCT-116 colon cancer cells to oxygen deprivation. Unlike cells harboring wild-type p53, p53-deficient HCT-116 cells were proven to be resistant to programmed cell death upon exposure to hypoxia. p53 has been previously reported to mediate the hypoxia-induced apoptosis by acting as a transrepressor for the anti-apoptotic protein ARC or as an inducer for pro-apoptotic targets such as Bnip3L<sup>132,133</sup>. In our present model we aimed to investigate the exact mechanism underlying both the p53-dependent and independent responses to hypoxia.

Ceramide has been regularly associated with p53 in the context of the response to cellular stress. However, the mechanisms underlying their coregulation were not fully characterized and largely depended on the cellular model and the type of the stress stimulus. In our present model of colon carcinoma, we demonstrated that in the absence of p53, HCT-116 cells resist hypoxia-induced apoptosis and increase ceramide levels. This phenomenon was not observed in p53-proficient cells, which suggests that ceramide accumulation in this model is independent of p53 and might contribute to the cellular resistance to hypoxic stress.

Since ceramide seems to work independently of p53 we concluded that either it is

completely dissociated from the cellular response to hypoxia, or it is partially catabolized into a prosurvival sphingolipid, promoting thereby the resistant phenotype in p53-deficient cells.

Ceramide accumulation in p53-deficient cells, observed through DGK assay and the analysis of the cellular sphingolipidome in response to oxygen deprivation, can be explained by an increase in ceramide generation or a decrease in ceramide catabolism. Analysis of the biosynthetic and catabolic pathways of ceramide metabolism through the administration of adequate inhibitors indicated that when inhibiting NSMase with GW4869 and inhibiting ASMase with desipramine no effect on the response of HCT-116 cells to hypoxia were observed, therefore we postulated that ceramide is dissociated from the cellular response to hypoxia.

In addition, when inhibiting CerSs with FB1, a slight decrease in the viability of p53-deficient cells was observed upon hypoxia. This suggests that ceramide generated through CerSs activity could contribute to the resistant phenotype observed in the absence of p53. Moreover, SK1 inhibition using SK1-I did not affect cell viability suggesting that S1P alone is not the only responsible for the prosurvival effects.

However, when blocking both CerSs and SK1, p53-deficient cells became sensitive to hypoxic stress and had decreased cellular viability compared to the vehicle-treated control.

It is noteworthy to mention that ceramide synthases partake in both the *de novo* sphingolipid synthesis, and the re-acylation of the free sphingosine recycled through the salvage pathway from pre-formed complex sphingolipids. When blocking ceramide synthases and SK1, which are key enzymes that occupy a unique niche in ceramide synthesis and breakdown respectively, the cell is left with sphingosine, a conventionally

established pro-apoptotic lipid<sup>133</sup>. Altering the sphingosine/S1P rheostat in favor of sphingosine in the p53-deficient cells might help sensitize these cells to hypoxia. Further experimental evidence is still needed to elucidate the detailed mechanism; one might suggest pre-treating HCT-116 cells with exogenous sphingosine and examining its effect on the p53-independent response to hypoxia.

In addition, knowing that ceramides harbor fatty acids with different chain lengths, several studies have indicated that some functions of ceramides are chain-length dependent. In studies published previously, it was shown that overexpression of C16-Cer in HCT-116 cells treated with Celecoxib induced pro-apoptotic effects<sup>134</sup>. In addition, overexpression of C24:0 and C24:1 in HeLa cells exposed to irradiation, resulted in anti-apoptotic effects. Whereas, overexpressed C16-Cer in the same irradiated cells induced pro-apoptotic effects<sup>135</sup>. In order to know which among ceramide species were being accumulated in p53-deficient cells upon hypoxic conditions, a detailed screening for ceramide species was performed by LC/MS to compare their distribution among p53-proficient and p53-deficient cells following oxygen deprivation. In fact, under physiological conditions, ceramide species were shown to be similarly distributed in p53-proficient and p53-deficient HCT-116 cells. However, this distribution was not the same upon exposure to chronic hypoxia. Our results showed a significant increase in the level of long and very long chain length ceramides in p53-deficient cells upon hypoxia. For example, the most abundant ceramide (C24:0) level was increased in p53-deficient cells upon chronic hypoxia by almost 3-fold compared to their normoxic time-matched control, while it was maintained in the p53-proficient cells. In studies performed on MCF-7 and HCT-116

cells, overexpression of CerS 4 and 6, responsible for long chain ceramides synthesis (C16:0, C18:0 and C20:0), inhibited cell proliferation and promoted apoptosis. In contrast, overexpression of CerS 2 accompanied with external addition of very long chain acyl-CoAs, thus increasing synthesis of very long chain ceramides, resulted in increased cell proliferation<sup>132</sup>.

Hence, one might conclude that the accumulation of long and very long chain ceramides, the bulk of which is C24:0 Cer, in p53-deficient cells upon exposure to chronic hypoxia may be responsible of cancer cell survival in p53-deficient HCT-116 cells as opposed to p53-proficient cells.

Previous work published by our team associated DEGS1 down regulation in the right ventricle of hypoxic animal models to the adaptive response to chronic hypoxia<sup>114,115,126</sup>. In contrast, in models of acute hypoxia, the *de novo* pathway of ceramide synthesis is activated driving apoptotic cell death<sup>117</sup>. In our present model, DEGS1 modulation seemed to take place after prolonged exposure to hypoxia (72 h). In the presence of p53, DEGS1 was down-regulated upon prolonged oxygen deprivation at the mRNA and protein levels, similarly to our previous findings in a p53-expressing chronic hypoxia model<sup>116,117,128</sup>. When p53 is lacking, DEGS1 expression was sustained in response to hypoxia, accompanied by an increase in ceramide levels (discussed above).

When tracking ceramide fate, we demonstrated that the basal level of sphingosine, assessed under normoxic conditions, was significantly higher in p53-deficient cells when compared to their p53-expressing counterparts, which was somehow expected. In fact, p53-deficient cells demonstrated a higher proliferative rate under physiological conditions and were likely to reach confluency earlier than the p53-expressing cell line.

When near confluency, the cells tend to recycle sphingolipids resulting in sphingosine generation. Upon 72 hours of exposure to hypoxia, p53-deficient cells demonstrated a decrease in the sphingosine level along with an increase in SK1 genomic expression. Altogether our data helped us hypothesize that under hypoxia, p53 negatively regulates ceramide metabolic pathways engendering apoptotic cell death. In contrast, p53-deficient cells were likely to overcome hypoxic stress by synthesizing ceramide through the *de novo* pathway, which was possibly deacylated into sphingosine that might have been phosphorylated by SK1 into S1P. Accumulating evidence has linked the SK1/S1P axis with the cellular adaptation to hypoxia, which corroborates our present findings<sup>136-138</sup>. Unfortunately, using the single-phase extraction method described by Bielawski<sup>139</sup>, we were not capable of detecting S1P by LC/MS, different type of lipid extraction will be investigated in the future.

Since S1P was solely linked to the adaptation to the decrease in oxygen supply whereas ceramide was associated with the hypoxic apoptosis<sup>117,140</sup>, we aimed to shift the sphingolipid balance toward a higher cellular ceramide/S1P ratio through the administration of synthetic cell-permeable short chain C6 ceramide. When reaching the inner cellular compartments, exogenous ceramide usually replaces the short 6 carbon fatty acid with a longer chain amplifying the pool of cellular ceramides, consequently driving apoptosis<sup>129,130</sup>. Our data highlighted the great potential of exogenous C6 ceramide administration in sensitizing p53-deficient cells to hypoxia-induced apoptosis. C6 ceramide promise in cancer therapy was also described in combination with various chemotherapeutic drugs including doxorubicin, paclitaxel (Taxol), histone deacetylase inhibitor, vincristine, pemetrexed, and others, which further supports the proposed strategy in hypoxic solid tumor systems where p53 is lacking<sup>141-146</sup>.

## CHAPTER V

### CONCLUSION AND PERSPECTIVES

Finally, we can conclude that the aggressive status of cancer cells is potentially linked to ceramide synthesis and its partial conversion to S1P in the p53-deficient cells upon exposure to hypoxia. Furthermore, our results shed the light on the role of exogenous C6 ceramide as an anti-cancer therapeutic strategy in p53-deficient tumors.

Based on these findings and the limitations that we faced, in the future perspectives we aim to:

- Measure S1P level using a suitable method of lipid extraction.
- Test the enzymatic activity of the three key enzymes that were shown to be involved in the response of HCT-116 cells to hypoxia: CerSs, DEGS1, and SK1.
- Evaluate the effect of DEGS1 pharmacological inhibition (using GT-11), alone and in combination with the SK1 inhibitor (SK1-I) on the response of both HCT-116 p53<sup>+/+</sup> and p53<sup>-/-</sup> cells to hypoxia.
- Validate the obtained results across a panel of p53-mutated cancer cell lines.
- Downregulate DEGS1 and SK1 expression in our cellular model through stably transfecting HCT-116 p53<sup>+/+</sup> and p53<sup>-/-</sup> cells with shRNA directed against *SphK1* and *DEGS1* genes, and evaluate the effect of gene knockdown on the

response to hypoxia *in vitro* and in the xenograft model established in BALB/c nu/nu mice.

- Encapsulate C6 ceramide into smart hypoxia-responsive nanoparticles (HRNPs) which will selectively release this bioactive lipid under hypoxic bio-reductive conditions. C6 ceramide-loaded HRNPs will be injected intravenously in BALB/c-nu/nu mice harboring HCT-116 xenografts differentially expressing p53. The tumor size will be monitored, and the molecular mechanisms underlying the response to hypoxia will be investigated.

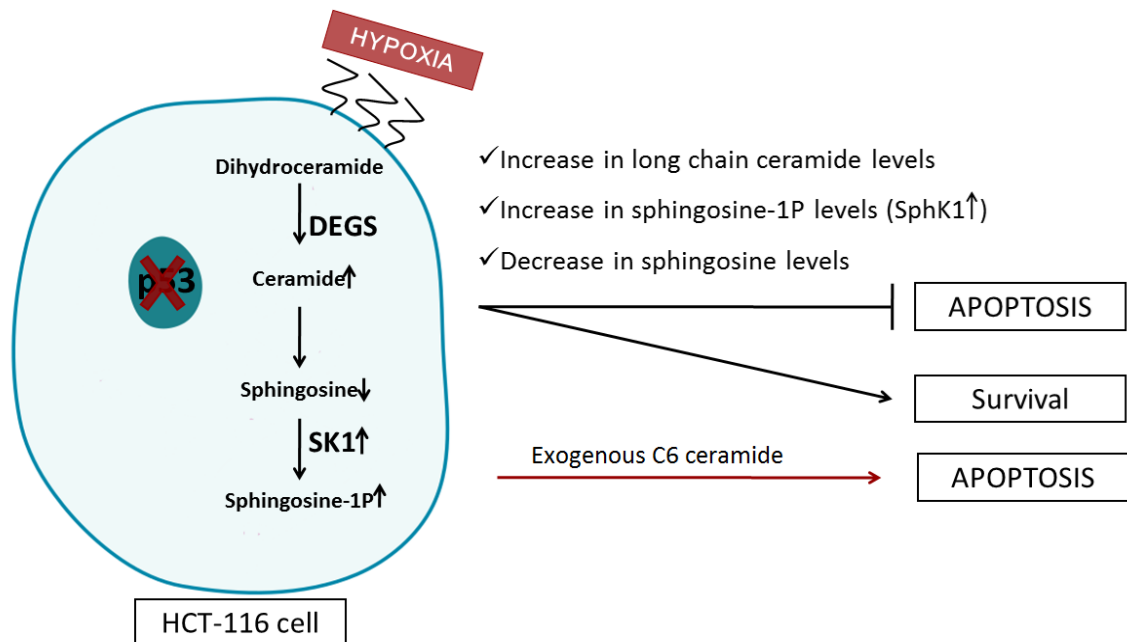


**Figure 22. Summary of possible changes in ceramide metabolism in response to hypoxia in HCT-116 p53<sup>-/-</sup> cells.** Once dihydroceramide is converted into ceramide through the enzyme DEGS1 in p53<sup>-/-</sup> HCT-116 cells upon hypoxia, ceramide is then probably converted into sphingosine which is possibly phosphorylated by the enzyme SK1 into the prosurvival sphingolipid S1P. In addition, the increase in long chain ceramide and the decrease in sphingosine might also be responsible for the resistance to hypoxia-induced apoptosis in the absence of p53. Administration of exogenous C6 ceramide reverted the hypoxia-resistant phenotype observed in p53<sup>-/-</sup> cells into an apoptotic one.



## BIBLIOGRAPHY

1. Cancer Facts & Figures 2020 | American Cancer Society.  
<https://www.cancer.org/research/cancer-facts-statistics/all-cancer-facts-figures/cancer-facts-figures-2020.html>.
2. Glover, M., Mansoor, E., Panhwar, M., Parasa, S. & Cooper, G. S. Epidemiology of Colorectal Cancer in Average Risk Adults 20–39 Years of Age: A Population-Based National Study. *Dig Dis Sci* **64**, 3602–3609 (2019).
3. Dekker, E., Tanis, P. J., Vleugels, J. L. A., Kasi, P. M. & Wallace, M. B. Colorectal cancer. *The Lancet* **394**, 1467–1480 (2019).
4. moph. <http://www.moph.gov.lb>.
5. Colorectal cancer: Epidemiology, risk factors, and protective factors - UpToDate.  
<https://www.uptodate.com/contents/colorectal-cancer-epidemiology-risk-factors-and-protective-factors>.
6. Keum, N. & Giovannucci, E. Global burden of colorectal cancer: emerging trends, risk factors and prevention strategies. *Nature Reviews Gastroenterology & Hepatology* **16**, 713–732 (2019).
7. Colorectal Cancer Risk Factors. <https://www.cancer.org/cancer/colon-rectal-cancer/causes-risks-prevention/risk-factors.html>.
8. Testa, U., Pelosi, E. & Castelli, G. Colorectal Cancer: Genetic Abnormalities, Tumor Progression, Tumor Heterogeneity, Clonal Evolution and Tumor-Initiating Cells. *Med Sci (Basel)* **6**, (2018).
9. Aran, V., Victorino, A. P., Thuler, L. C. & Ferreira, C. G. Colorectal Cancer: Epidemiology, Disease Mechanisms and Interventions to Reduce Onset and Mortality. *Clin Colorectal Cancer* **15**, 195–203 (2016).

10. Nakayama, M. & Oshima, M. Mutant p53 in colon cancer. *J Mol Cell Biol* **11**, 267–276 (2018).
11. Yamagishi, H., Kuroda, H., Imai, Y. & Hiraishi, H. Molecular pathogenesis of sporadic colorectal cancers. *Chin J Cancer* **35**, (2016).
12. Nguyen, H. T. & Duong, H.-Q. The molecular characteristics of colorectal cancer: Implications for diagnosis and therapy. *Oncol Lett* **16**, 9–18 (2018).
13. Walther, A. *et al.* Genetic prognostic and predictive markers in colorectal cancer. *Nat Rev Cancer* **9**, 489–499 (2009).
14. Lane, D. P. Cancer. p53, guardian of the genome. *Nature* **358**, 15–16 (1992).
15. Reference, G. H. TP53 gene. *Genetics Home Reference*  
<https://ghr.nlm.nih.gov/gene/TP53>.
16. Kasthuber, E. & Lowe, S. Putting p53 in context. *Cell* **170**, 1062–1078 (2017).
17. Toufekchan, E. & Toledo, F. The Guardian of the Genome Revisited: p53 Downregulates Genes Required for Telomere Maintenance, DNA Repair, and Centromere Structure. *Cancers (Basel)* **10**, (2018).
18. Sullivan, K. D., Galbraith, M. D., Andrysiak, Z. & Espinosa, J. M. Mechanisms of transcriptional regulation by p53. *Cell Death Differ.* **25**, 133–143 (2018).
19. Liu, J., Zhang, C., Hu, W. & Feng, Z. Tumor suppressor p53 and metabolism. *J Mol Cell Biol* **11**, 284–292 (2019).
20. Aubrey, B. J., Kelly, G. L., Janic, A., Herold, M. J. & Strasser, A. How does p53 induce apoptosis and how does this relate to p53-mediated tumour suppression? *Cell Death Differ.* **25**, 104–113 (2018).

21. Zeng, H. *et al.* DNA Checkpoint and Repair Factors Are Nuclear Sensors for Intracellular Organelle Stresses—Inflammations and Cancers Can Have High Genomic Risks. *Front. Physiol.* **9**, (2018).
22. Chen, J. The Cell-Cycle Arrest and Apoptotic Functions of p53 in Tumor Initiation and Progression. *Cold Spring Harb Perspect Med* **6**, (2016).
23. ter Huurne, M. *et al.* Critical Role for P53 in Regulating the Cell Cycle of Ground State Embryonic Stem Cells. *Stem Cell Reports* **14**, 175–183 (2020).
24. Lieschke, E., Wang, Z., Kelly, G. L. & Strasser, A. Discussion of some ‘knowns’ and some ‘unknowns’ about the tumour suppressor p53. *J Mol Cell Biol* **11**, 212–223 (2019).
25. Haupt, S., Berger, M., Goldberg, Z. & Haupt, Y. Apoptosis - the p53 network. *Journal of Cell Science* **116**, 4077–4085 (2003).
26. Belkacemi, L. Exploiting the Extrinsic and the Intrinsic Apoptotic Pathways for Cancer Therapeutics. *Journal of Cancer & Cure* **1**, (2018).
27. Vieler, M. & Sanyal, S. p53 Isoforms and Their Implications in Cancer. *Cancers (Basel)* **10**, (2018).
28. Mantovani, F., Collavin, L. & Del Sal, G. Mutant p53 as a guardian of the cancer cell. *Cell Death Differ.* **26**, 199–212 (2019).
29. Nakayama, M. & Oshima, M. Mutant p53 in colon cancer. *J Mol Cell Biol* **11**, 267–276 (2019).
30. Larson, C. *et al.* Going viral: a review of replication-selective oncolytic adenoviruses. *Oncotarget* **6**, 19976–19989 (2015).

31. Zhao, Y., Aguilar, A., Bernard, D. & Wang, S. Small-Molecule Inhibitors of the MDM2–p53 Protein–Protein Interaction (MDM2 Inhibitors) in Clinical Trials for Cancer Treatment. *J Med Chem* **58**, 1038–1052 (2015).
32. Martins, C. P., Brown-Swigart, L. & Evan, G. I. Modeling the therapeutic efficacy of p53 restoration in tumors. *Cell* **127**, 1323–1334 (2006).
33. Ventura, A. *et al.* Restoration of p53 function leads to tumour regression in vivo. *Nature* **445**, 661–665 (2007).
34. Xue, W. *et al.* Senescence and tumour clearance is triggered by p53 restoration in murine liver carcinomas. *Nature* **445**, 656–660 (2007).
35. Kastan, M. B. Wild-type p53: tumors can't stand it. *Cell* **128**, 837–840 (2007).
36. Vermeij, R. *et al.* Immunological and Clinical Effects of Vaccines Targeting p53-Overexpressing Malignancies. *J Biomed Biotechnol* **2011**, (2011).
37. Gavhan, Y. N., Shete, A. S., Bhagat, A. K. & Shinde, V. R. Solid Tumors: Facts, Challenges and Solutions. *Int. J. Pharm. Sci.*
38. How Fast Does Cancer Spread? Without Treatment, Growth Rate, More. <https://www.healthline.com/health/cancer/how-fast-does-cancer-spread>.
39. Cancer Cells vs Normal Cells. *Cancer Research from Technology Networks* <https://www.technologynetworks.com/cancer-research/articles/cancer-cells-vs-normal-cells-307366>.
40. Cell Signaling in Cancer. *Cancer Research from Technology Networks* <https://www.technologynetworks.com/cancer-research/articles/cell-signaling-in-cancer-313171>.

41. Martin, J. D., Fukumura, D., Duda, D. G., Boucher, Y. & Jain, R. K. Reengineering the Tumor Microenvironment to Alleviate Hypoxia and Overcome Cancer Heterogeneity. *Cold Spring Harb Perspect Med* **6**, (2016).
42. Li, T., Kang, G., Wang, T. & Huang, H. Tumor angiogenesis and anti-angiogenic gene therapy for cancer. *Oncol Lett* **16**, 687–702 (2018).
43. Martin, J. D., Seano, G. & Jain, R. K. Normalizing Function of Tumor Vessels: Progress, Opportunities, and Challenges. *Annu Rev Physiol* **81**, 505–534 (2019).
44. Zuazo-Gaztelu, I. & Casanovas, O. Unraveling the Role of Angiogenesis in Cancer Ecosystems. *Front. Oncol.* **8**, (2018).
45. Graham, K. & Unger, E. Overcoming tumor hypoxia as a barrier to radiotherapy, chemotherapy and immunotherapy in cancer treatment. *Int J Nanomedicine* **13**, 6049–6058 (2018).
46. Bertout, J. A., Patel, S. A. & Simon, M. C. The impact of O<sub>2</sub> availability on human cancer. *Nat. Rev. Cancer* **8**, 967–975 (2008).
47. Challapalli, A., Carroll, L. & Aboagye, E. O. Molecular mechanisms of hypoxia in cancer. *Clin Transl Imaging* **5**, 225–253 (2017).
48. Humpton, T. J. & Vousden, K. H. Regulation of Cellular Metabolism and Hypoxia by p53. *Cold Spring Harb Perspect Med* **6**, (2016).
49. Wang, P., Guan, D., Zhang, X.-P., Liu, F. & Wang, W. Modeling the regulation of p53 activation by HIF-1 upon hypoxia. *FEBS Letters* **593**, 2596–2611 (2019).
50. Pezzuto, A. & Carico, E. Role of HIF-1 in Cancer Progression: Novel Insights. A Review. *Curr. Mol. Med.* **18**, 343–351 (2018).
51. Choudhry, H. & Harris, A. L. Advances in Hypoxia-Inducible Factor Biology. *Cell Metabolism* **27**, 281–298 (2018).

52. Soni, S. & Padwad, Y. S. HIF-1 in cancer therapy: two decade long story of a transcription factor. *Acta Oncol* **56**, 503–515 (2017).
53. Koyasu, S., Kobayashi, M., Goto, Y., Hiraoka, M. & Harada, H. Regulatory mechanisms of hypoxia-inducible factor 1 activity: Two decades of knowledge. *Cancer Sci.* **109**, 560–571 (2018).
54. Obacz, J., Pastorekova, S., Vojtesek, B. & Hrstka, R. Cross-talk between HIF and p53 as mediators of molecular responses to physiological and genotoxic stresses. *Molecular Cancer* **12**, 93 (2013).
55. Schmid, T., Zhou, J. & Brüne, B. HIF-1 and p53: communication of transcription factors under hypoxia. *J. Cell. Mol. Med.* **8**, 423–431 (2004).
56. Leszczynska, K. B. *et al.* Hypoxia-induced p53 modulates both apoptosis and radiosensitivity via AKT. *J Clin Invest* **125**, 2385–2398 (2015).
57. Gogna, R., Madan, E., Kuppusamy, P. & Pati, U. Re-oxygenation causes hypoxic tumor regression through restoration of p53 wild-type conformation and post-translational modifications. *Cell Death Dis* **3**, e286 (2012).
58. Nardinocchi, L., Puca, R., Givol, D. & D’Orazi, G. HIPK2-a therapeutical target to be (re)activated for tumor suppression: role in p53 activation and HIF-1 $\alpha$  inhibition. *Cell Cycle* **9**, 1270–1275 (2010).
59. Nardinocchi, L. *et al.* Targeting hypoxia in cancer cells by restoring homeodomain interacting protein-kinase 2 and p53 activity and suppressing HIF-1 $\alpha$ . *PLoS ONE* **4**, e6819 (2009).
60. Mencarelli, C. & Martinez-Martinez, P. Ceramide function in the brain: when a slight tilt is enough. *Cell. Mol. Life Sci.* **70**, 181–203 (2013).

61. Ogretmen, B. Sphingolipid metabolism in cancer signalling and therapy. *Nat Rev Cancer* **18**, 33–50 (2018).
62. Sokolowska, E. & Blachnio-Zabielska, A. The Role of Ceramides in Insulin Resistance. *Front. Endocrinol.* **10**, (2019).
63. Turpin-Nolan, S. M. & Brüning, J. C. The role of ceramides in metabolic disorders: when size and localization matters. *Nature Reviews Endocrinology* 1–10 (2020) doi:10.1038/s41574-020-0320-5.
64. García-González, V. *et al.* Ceramide Metabolism Balance, a Multifaceted Factor in Critical Steps of Breast Cancer Development. *Int J Mol Sci* **19**, (2018).
65. Mashhadi Akbar Boojar, M., Mashhadi Akbar Boojar, M. & Golmohammad, S. Ceramide pathway: A novel approach to cancer chemotherapy. *Egyptian Journal of Basic and Applied Sciences* **5**, 237–244 (2018).
66. Reynolds, C. P., Maurer, B. J. & Kolesnick, R. N. Ceramide synthesis and metabolism as a target for cancer therapy. *Cancer Lett.* **206**, 169–180 (2004).
67. Hage-Sleiman, R., Esmerian, M. O., Kobeissy, H. & Dbaibo, G. p53 and Ceramide as Collaborators in the Stress Response. *Int J Mol Sci* **14**, 4982–5012 (2013).
68. Cha, H. J. *et al.* Intercellular and intracellular functions of ceramides and their metabolites in skin (Review). *Int. J. Mol. Med.* **38**, 16–22 (2016).
69. Wigger, D., Gulbins, E., Kleuser, B. & Schumacher, F. Monitoring the Sphingolipid de novo Synthesis by Stable-Isotope Labeling and Liquid Chromatography-Mass Spectrometry. *Front. Cell Dev. Biol.* **7**, (2019).
70. Bandet, C. L. *et al.* Ceramide Transporter CERT Is Involved in Muscle Insulin Signaling Defects Under Lipotoxic Conditions. *Diabetes* **67**, 1258–1271 (2018).

71. Liu, L.-K., Choudhary, V., Toulmay, A. & Prinz, W. A. An inducible ER–Golgi tether facilitates ceramide transport to alleviate lipotoxicity. *J Cell Biol* **216**, 131–147 (2017).
72. Riley, R. T. & Merrill, A. H. Ceramide synthase inhibition by fumonisins: a perfect storm of perturbed sphingolipid metabolism, signaling and disease. *J. Lipid Res.* jlr.S093815 (2019) doi:10.1194/jlr.S093815.
73. Espaillet, M. P., Shamseddine, A. A., Adada, M. M., Hannun, Y. A. & Obeid, L. M. Ceramide and sphingosine-1-phosphate in cancer, two faces of the sphinx. *Translational Cancer Research* **4**, 484–499 (2015).
74. Levy, M. & Futerman, A. H. Mammalian Ceramide Synthases. *IUBMB Life* **62**, 347–356 (2010).
75. Fabrias, G. *et al.* Dihydroceramide desaturase and dihydrosphingolipids: Debutant players in the sphingolipid arena. *Progress in Lipid Research* **51**, 82–94 (2012).
76. Rodriguez-Cuenca, S., Barbarroja, N. & Vidal-Puig, A. Dihydroceramide desaturase 1, the gatekeeper of ceramide induced lipotoxicity. *Biochim. Biophys. Acta* **1851**, 40–50 (2015).
77. Andrieu-Abadie, N. & Levade, T. Sphingomyelin hydrolysis during apoptosis. *Biochim. Biophys. Acta* **1585**, 126–134 (2002).
78. Ueda, N. Ceramide-induced apoptosis in renal tubular cells: a role of mitochondria and sphingosine-1-phosphate. *Int J Mol Sci* **16**, 5076–5124 (2015).
79. Di Pardo, A. & Maglione, V. Sphingolipid Metabolism: A New Therapeutic Opportunity for Brain Degenerative Disorders. *Front Neurosci* **12**, 249 (2018).



80. Brodowicz, J., Przegaliński, E., Müller, C. P. & Filip, M. Ceramide and Its Related Neurochemical Networks as Targets for Some Brain Disorder Therapies. *Neurotox Res* **33**, 474–484 (2018).
81. Parveen, F. *et al.* Role of Ceramidases in Sphingolipid Metabolism and Human Diseases. *Cells* **8**, 1573 (2019).
82. Pralhada Rao, R. *et al.* Sphingolipid Metabolic Pathway: An Overview of Major Roles Played in Human Diseases. *Journal of Lipids*  
<https://www.hindawi.com/journals/jl/2013/178910/> (2013)  
doi:<https://doi.org/10.1155/2013/178910>.
83. Kitatani, K., Idkowiak-Baldys, J. & Hannun, Y. A. The sphingolipid salvage pathway in ceramide metabolism and signaling. *Cell. Signal.* **20**, 1010–1018 (2008).
84. Lewis, A. C., Wallington-Beddoe, C. T., Powell, J. A. & Pitson, S. M. Targeting sphingolipid metabolism as an approach for combination therapies in haematological malignancies. *Cell Death Discovery* **4**, 1–11 (2018).
85. Knapp, P., Chomicz, K., Świdarska, M., Chabowski, A. & Jach, R. Unique Roles of Sphingolipids in Selected Malignant and Nonmalignant Lesions of Female Reproductive System. *BioMed Research International*  
<https://www.hindawi.com/journals/bmri/2019/4376583/> (2019)  
doi:<https://doi.org/10.1155/2019/4376583>.
86. Zitomer, N. C. *et al.* Ceramide Synthase Inhibition by Fumonisin B1 Causes Accumulation of 1-Deoxysphinganine. *J Biol Chem* **284**, 4786–4795 (2009).

87. Smith, G. W. Chapter 71 - Fumonisin. in *Veterinary Toxicology (Third Edition)* (ed. Gupta, R. C.) 1003–1018 (Academic Press, 2018). doi:10.1016/B978-0-12-811410-0.00071-4.
88. Riley, R. T. & Merrill, A. H. Ceramide synthase inhibition by fumonisins: a perfect storm of perturbed sphingolipid metabolism, signaling and disease. *J. Lipid Res.* jlr.S093815 (2019) doi:10.1194/jlr.S093815.
89. Cockburn, C. L. *et al.* Functional inhibition of acid sphingomyelinase disrupts infection by intracellular bacterial pathogens. *Life Sci Alliance* **2**, (2019).
90. Beckmann, N., Sharma, D., Gulbins, E., Becker, K. A. & Edelmann, B. Inhibition of acid sphingomyelinase by tricyclic antidepressants and analogs. *Front Physiol* **5**, 331 (2014).
91. Aslan, M., Özcan, F., Tuzcu, H., Kıraç, E. & Elpek, G. O. Inhibition of neutral sphingomyelinase decreases arachidonic acid mediated inflammation in liver ischemia-reperfusion injury. *Int J Clin Exp Pathol* **7**, 7814–7823 (2014).
92. Airola, M. *et al.* Structure of human nSMase2 reveals an interdomain allosteric activation mechanism for ceramide generation. *Proceedings of the National Academy of Sciences* **114**, 201705134 (2017).
93. Cao, M. *et al.* Sphingosine kinase inhibitors: A patent review. *International Journal of Molecular Medicine* **41**, 2450–2460 (2018).
94. Lynch, K. R., Thorpe, S. B. & Santos, W. L. Sphingosine kinase inhibitors: a review of patent literature (2006–2015). *Expert Opin Ther Pat* **26**, 1409–1416 (2016).
95. Wattenberg, B. W. The long and the short of ceramides. *J Biol Chem* **293**, 9922–9923 (2018).

96. Saddoughi, S. A., Song, P. & Ogretmen, B. Roles of bioactive sphingolipids in cancer biology and therapeutics. *Subcell. Biochem.* **49**, 413–440 (2008).
97. Jeffries, K. A. & Krupenko, N. I. Ceramide Signaling and p53 Pathways. *Adv. Cancer Res.* **140**, 191–215 (2018).
98. Schiffmann, S. *et al.* Ceramide synthases and ceramide levels are increased in breast cancer tissue. *Carcinogenesis* **30**, 745–752 (2009).
99. Siddique, M. M., Li, Y., Chaurasia, B., Kaddai, V. A. & Summers, S. A. Dihydroceramides: From Bit Players to Lead Actors. *J Biol Chem* **290**, 15371–15379 (2015).
100. Ogretmen, B. & Hannun, Y. A. Updates on functions of ceramide in chemotherapy-induced cell death and in multidrug resistance. *Drug Resist. Updat.* **4**, 368–377 (2001).
101. Chakraborty, P. *et al.* Pro-Survival Lipid Sphingosine-1-Phosphate Metabolically Programs T Cells to Limit Anti-tumor Activity. *Cell Rep* **28**, 1879-1893.e7 (2019).
102. Gouazé-Andersson, V. *et al.* Inhibition of acid ceramidase by a 2-substituted aminoethanol amide synergistically sensitizes prostate cancer cells to N-(4-hydroxyphenyl) retinamide. *Prostate* **71**, 1064–1073 (2011).
103. Gao, Y., Gao, F., Chen, K., Tian, M. & Zhao, D. Sphingosine kinase 1 as an anticancer therapeutic target. *Drug Des Devel Ther* **9**, 3239–3245 (2015).
104. Ma, Y.-Y., Mou, X.-Z., Ding, Y.-H., Zou, H. & Huang, D.-S. Delivery systems of ceramide in targeted cancer therapy: ceramide alone or in combination with other anti-tumor agents. *Expert Opin Drug Deliv* **13**, 1397–1406 (2016).
105. Minarowska, A., Minarowski, L., Karwowska, A. & Gacko, M. Regulatory role of cathepsin D in apoptosis. *Folia Histochem. Cytobiol.* **45**, 159–163 (2007).

106. Pruschy, M. *et al.* Ceramide triggers p53-dependent apoptosis in genetically defined fibrosarcoma tumour cells. *Br. J. Cancer* **80**, 693–698 (1999).
107. Dbaibo, G. S. *et al.* p53-dependent ceramide response to genotoxic stress. *J. Clin. Invest.* **102**, 329–339 (1998).
108. Panjarian, S. *et al.* De novo N-palmitoylsphingosine synthesis is the major biochemical mechanism of ceramide accumulation following p53 up-regulation. *Prostaglandins Other Lipid Mediat.* **86**, 41–48 (2008).
109. Dbaibo, G. S., Obeid, L. M. & Hannun, Y. A. The Role of Ceramide in the Cellular Stress Response. in *Frontiers in Bioactive Lipids* (ed. Vanderhoek, J. Y.) 183–192 (Springer US, 1996). doi:10.1007/978-1-4615-5875-0\_25.
110. Stith, J. L., Velazquez, F. N. & Obeid, L. M. Advances in determining signaling mechanisms of ceramide and role in disease. *J. Lipid Res.* jlr.S092874 (2019) doi:10.1194/jlr.S092874.
111. Liu, J., Beckman, B. S. & Foroozesh, M. A review of ceramide analogs as potential anticancer agents. *Future Med Chem* **5**, 1405–1421 (2013).
112. Tong, W.-W., Tong, G.-H. & Liu, Y. Cancer stem cells and hypoxia-inducible factors (Review). *Int. J. Oncol.* **53**, 469–476 (2018).
113. Padmanabha, D. HIF-INDEPENDENT RESPONSES IN HYPOXIA. *Theses and Dissertations* (2015) doi:<https://doi.org/10.25772/PYJY-PW08>.
114. Azzam, R. *et al.* Regulation of de novo ceramide synthesis: the role of dihydroceramide desaturase and transcriptional factors NFATC and Hand2 in the hypoxic mouse heart. *DNA Cell Biol.* **32**, 310–319 (2013).

115. Nouredine, L. *et al.* Modulation of total ceramide and constituent ceramide species in the acutely and chronically hypoxic mouse heart at different ages. *Prostaglandins Other Lipid Mediat* **86**, 49–55 (2008).
116. Devlin, C. M. *et al.* Dihydroceramide-based Response to Hypoxia. *J. Biol. Chem.* **286**, 38069–38078 (2011).
117. Kang, M. S. *et al.* Hypoxia-induced neuronal apoptosis is mediated by de novo synthesis of ceramide through activation of serine palmitoyltransferase. *Cell. Signal.* **22**, 610–618 (2010).
118. Greenblatt, M. S., Bennett, W. P., Hollstein, M. & Harris, C. C. Mutations in the p53 Tumor Suppressor Gene: Clues to Cancer Etiology and Molecular Pathogenesis. *Cancer Res* **54**, 4855–4878 (1994).
119. Dittmer, D. *et al.* Gain of function mutations in p53. *Nat. Genet.* **4**, 42–46 (1993).
120. Zalcenstein, A. *et al.* Mutant p53 gain of function: repression of CD95(Fas/APO-1) gene expression by tumor-associated p53 mutants. *Oncogene* **22**, 5667–5676 (2003).
121. Wong, R. P. C. *et al.* p53-R273H gains new function in induction of drug resistance through down-regulation of procaspase-3. *Molecular Cancer Therapeutics* **6**, 1054–1061 (2007).
122. Bossi, G. *et al.* Mutant p53 gain of function: reduction of tumor malignancy of human cancer cell lines through abrogation of mutant p53 expression. *Oncogene* **25**, 304–309 (2006).
123. Graeber, T. G. *et al.* Hypoxia induces accumulation of p53 protein, but activation of a G1-phase checkpoint by low-oxygen conditions is independent of p53 status. *Mol. Cell. Biol.* **14**, 6264–6277 (1994).

124. Graeber, T. G. *et al.* Hypoxia-mediated selection of cells with diminished apoptotic potential in solid tumours. *Nature* **379**, 88–91 (1996).
125. Bligh, E. G. & Dyer, W. J. A Rapid Method of Total Lipid Extraction and Purification. *Can. J. Biochem. Physiol.* **37**, 911–917 (1959).
126. Bitar, F. F. *et al.* Modulation of ceramide content and lack of apoptosis in the chronically hypoxic neonatal rat heart. *Pediatr. Res.* **51**, 144–149 (2002).
127. Law, B. A. *et al.* Lipotoxic very-long-chain ceramides cause mitochondrial dysfunction, oxidative stress, and cell death in cardiomyocytes. *The FASEB Journal* **32**, 1403–1416 (2018).
128. Selvam, S. P. & Ogretmen, B. Sphingosine kinase/sphingosine 1-phosphate signaling in cancer therapeutics and drug resistance. *Handb Exp Pharmacol* 3–27 (2013) doi:10.1007/978-3-7091-1511-4\_1.
129. Ogretmen, B. *et al.* Biochemical mechanisms of the generation of endogenous long chain ceramide in response to exogenous short chain ceramide in the A549 human lung adenocarcinoma cell line. Role for endogenous ceramide in mediating the action of exogenous ceramide. *J. Biol. Chem.* **277**, 12960–12969 (2002).
130. Takeda, S., Mitsutake, S., Tsuji, K. & Igarashi, Y. Apoptosis occurs via the ceramide recycling pathway in human HaCaT keratinocytes. *J. Biochem.* **139**, 255–262 (2006).
131. Graeber, T. G. *et al.* Hypoxia-mediated selection of cells with diminished apoptotic potential in solid tumours. *Nature* **379**, 88–91 (1996).
132. Hartmann, D. *et al.* Long chain ceramides and very long chain ceramides have opposite effects on human breast and colon cancer cell growth. *The International Journal of Biochemistry & Cell Biology* **44**, 620–628 (2012).

133. Cuvillier, O. Sphingosine in apoptosis signaling. *Biochim. Biophys. Acta* **1585**, 153–162 (2002).
134. Schiffmann, S. *et al.* Activation of ceramide synthase 6 by celecoxib leads to a selective induction of C16:0-ceramide. *Biochem. Pharmacol.* **80**, 1632–1640 (2010).
135. Mesicek, J. *et al.* Ceramide synthases 2, 5, and 6 confer distinct roles in radiation-induced apoptosis in HeLa cells. *Cell. Signal.* **22**, 1300–1307 (2010).
136. Karliner, J. S., Honbo, N., Summers, K., Gray, M. O. & Goetzl, E. J. The lysophospholipids sphingosine-1-phosphate and lysophosphatidic acid enhance survival during hypoxia in neonatal rat cardiac myocytes. *J. Mol. Cell. Cardiol.* **33**, 1713–1717 (2001).
137. Zhang, J. *et al.* Signals from type 1 sphingosine 1-phosphate receptors enhance adult mouse cardiac myocyte survival during hypoxia. *American Journal of Physiology-Heart and Circulatory Physiology* **293**, H3150–H3158 (2007).
138. Zhang, H. *et al.* Inhibition of sphingosine kinase 1 suppresses proliferation of glioma cells under hypoxia by attenuating activity of extracellular signal-regulated kinase. *Cell Prolif.* **45**, 167–175 (2012).
139. Bielawski, J. *et al.* Comprehensive quantitative analysis of bioactive sphingolipids by high-performance liquid chromatography-tandem mass spectrometry. *Methods Mol. Biol.* **579**, 443–467 (2009).
140. Maurer, B. J., Metelitsa, L. S., Seeger, R. C., Cabot, M. C. & Reynolds, C. P. Increase of Ceramide and Induction of Mixed Apoptosis/Necrosis by N-(4-Hydroxyphenyl)-retinamide in Neuroblastoma Cell Lines. *J Natl Cancer Inst* **91**, 1138–1146 (1999).

141. Chen, M.-B. *et al.* C6 ceramide dramatically increases vincristine sensitivity both in vivo and in vitro, involving AMP-activated protein kinase-p53 signaling. *Carcinogenesis* **36**, 1061–1070 (2015).
142. Ji, C. *et al.* Exogenous cell-permeable C6 ceramide sensitizes multiple cancer cell lines to Doxorubicin-induced apoptosis by promoting AMPK activation and mTORC1 inhibition. *Oncogene* **29**, 6557–6568 (2010).
143. Yang, L. *et al.* C6 ceramide dramatically enhances docetaxel-induced growth inhibition and apoptosis in cultured breast cancer cells: a mechanism study. *Exp. Cell Res.* **332**, 47–59 (2015).
144. Yu, T., Li, J. & Sun, H. C6 ceramide potentiates curcumin-induced cell death and apoptosis in melanoma cell lines in vitro. *Cancer Chemother. Pharmacol.* **66**, 999–1003 (2010).
145. Zhu, Q. -y *et al.* C6-ceramide synergistically potentiates the anti-tumor effects of histone deacetylase inhibitors via AKT dephosphorylation and  $\alpha$ -tubulin hyperacetylation both in vitro and in vivo. *Cell Death Dis* **2**, e117 (2011).
146. Zhu, X. *et al.* C6 ceramide sensitizes pemetrexed-induced apoptosis and cytotoxicity in osteosarcoma cells. *Biochemical and Biophysical Research Communications* **452**, 72–78 (2014).